



Electromagnetic field analysis of shielded composite dielectric spherical shell resonator in infrared and visible regions

D.P. Yadav^a, M.K. Maurya^{b,*}, R.A. Yadav^c

^a Department of Physics, Udai Pratap Autonomous P.G. College, Varanasi 221002, U.P., India

^b Department of Physics, Rajeev Gandhi Government P.G. College, Ambikapur 497001, Chhattisgarh, India

^c Department of Physics, Banaras Hindu University, Varanasi 221005, U.P., India

ARTICLE INFO

Article history:

Received 28 May 2018

Revised 28 November 2018

Accepted 1 December 2018

Available online 3 December 2018

Keywords:

Shielded composite dielectric spherical shell resonator

Normal modes

Resonant frequencies and quality factor

ABSTRACT

In this paper, we have presented an electromagnetic field analysis of shielded composite dielectric spherical shell resonator. The resonator studied in this work is considered for the first time as no study on such resonators is available in the published literature to the best of the author's information. This shielded composite dielectric spherical shell resonator is composed of two concentric metal spheres with different dielectric material has been made. The whole assembly is shielded by a perfectly conducting concentric spherical metal. The expression for the resonant frequencies and quality factors have been calculated using numerical methods for both the $TE_{nm\ell}$ and $TM_{nm\ell}$ modes for an infrared and visible regions. It is found that as the outer radius of the shielded composite dielectric spherical shell resonator increases, the quality factor Q of the resonator increases monotonically. It is also found that if we change the radius of the inner dielectric sphere, there is no appreciable change in resonant frequency of the concerned mode is observed. This is due to the small difference in the permittivities of the materials of the inner and the outer dielectric spheres. It has also been observed that an inner concentric superconducting sphere within a dielectric spherical resonator is a more effective controlling parameter of the resonant frequency than the other parameters.

© 2018 Elsevier Ltd. All rights reserved.

1. Introduction

In recent years, with the advent of new materials with both permittivity and quality factor as well as low temperature coefficient, a progressive effort in the miniaturization and stabilization of components for applications in microwaves and millimeter waves such as oscillators, dielectric loaded resonators, and filters has been made [1–5]. Resonators are important components in microwave communication systems. These are used as filters, oscillators, amplifiers, and tuners. Fields inside a resonator store energy at the resonant frequency where equal storage of electric and magnetic energies occurs [3–14].

Dielectric resonators (DRs) for millimeter wave frequencies demand the use of very small dielectric devices. The manufacture of these micro-resonators recommends the use of geometries such as spheres or hemispheres which are easier to produce than rod or ring shapes [4–10]. These kinds of dielectric samples can be inserted in to micro-strip structures to design passive circuits such as

filters or to couple with active circuits to stabilize the resonant frequency of oscillators [7,12–16]. When they work with azimuthally high order modes of whispering gallery modes (WGM), they are applied in the design of ultra stable oscillators and in the studies of new dielectric materials [9–17].

Several approaches to analyze these DRs can be found in literature, such as the dielectric wave guide method [18], the radial mode-matching method by Kobayashi and Tanaka [19], or the axial mode-matching method by Zoki and Atia [20], as well as a method based on the surface integral equation techniques [4] or the asymptotic expansion method [21]. When the shape of the DR is complex, a geometrically flexible numerical method such as finite element method (FEM) might be advantageous. Some formulations based on finite elements have been applied to the study of axisymmetric dielectric resonators in cavities like [23–26].

The effort to improve microwave resonator performance, as measured by the device Q -factor, has caused an evolution to occur in the fundamental structure of the physical resonator [6,9,13]. Simple metal cavity resonators, where the enclosure wall losses determine the achievable Q , were superseded by dielectric loaded cavities which attained higher Q 's by confining more of the field of the resonant mode away from the lossy enclosure walls [17–26].

* Corresponding author.

E-mail address: mahendrabhu@gmail.com (M.K. Maurya).

Spherical cavity resonator is a spherical metallic cavity. Electromagnetic field analysis for such a resonator has been presented in standard texts wherein resonant frequencies have been computed for the microwave region of the electromagnetic spectrum [1–12]. Spherical cavity resonator may be filled with a dielectric medium which becomes a shielded spherical dielectric resonator [8–11].

Dielectric resonators made of crystalline materials such as quartz or sapphire with a high Q -factor and good temperature stability have also been considered. Studies on uniaxially anisotropic dielectric resonators have been reported in literatures [27,28], where in only modes with no or a low order of azimuthal variations have been considered. An attempt at describing these anisotropic resonators operating at azimuthal higher order modes, called whispering gallery modes (WGMs), has been made [26–40].

In some applications, or to compensate for the deviations as a result of mechanical tolerances, tunable resonators might be required. Typical tuning elements are metallic screws, plates moving toward dielectric resonator, or dielectric devices [4–23].

High- Q dielectric resonators have also been used as stabilizing devices for oscillators in microwave integrated circuits. Resonant frequencies, field distributions and Q -factors for modes with a no azimuthal variation ($m=0$), hybrid modes ($m \neq 0$), or even modes with a high azimuthal variation (WGM) in dielectric resonators on microstrip substrates or supporters, and with or without tuning devices, have to be efficiently obtained. For application in microwave region reduction in the size of the dielectric resonators has focused the attention of the researchers toward new shapes such as spherical or hemispherical resonators. A dielectric sphere resonator on a substrate into a cylindrical conducting cavity together with a conical resonator structure was studied [18], where, the mode-matching method was used and these geometries were simulated by bodies of revolution with stepped cross sections, where many steps and a modal convergence study is necessary; furthermore, resonant frequencies of hybrid modes and quality factors were not computed.

Spherical resonators operating in WGMs achieve high quality-factor values and can be used to stabilize integrated oscillators. As a consequence of spherical symmetry, a spherical resonator has a large spherical density of WGMs which is not appropriate for a single-mode operation. Furthermore, the spherical shape can be mechanically unstable. Hemispherical resonators have a lower spectral density though their unloaded Q -factor becomes a little smaller. An image hemispherical dielectric resonator with WGM, used as an oscillator system for millimeter devices, has been investigated by Kharkovsky et al. [36]. The hemispherical DR is also used to design dielectric-resonator antennas (DRAs) as an alternative to microstrip antennas [32–41] has studied cylindrical and spherical dielectric resonators in cavities and microwave integrated circuits, using finite elements method.

In the present paper, we have theoretically analyzed the normal modes and quality factors for composite shielded dielectric spherical shell resonator with a concentric metallic sphere at the centre in infrared and visible regions. In the earlier published literature [8–26,33–40], computation of these factors parameters for composite shielded dielectric spherical shell resonator with a concentric metallic sphere has not been explored in details. The resonant frequencies and quality factors have been calculated using analytical expressions for both the $TE_{nm\ell}$ and $TM_{nm\ell}$ modes in an infrared and visible regions.

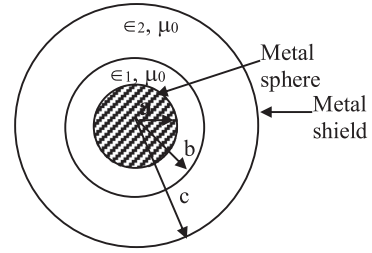


Fig. 1. Shielded composite dielectric spherical shell resonator with a metallic sphere of radius a at the centre and enclosed in a metallic spherical shell of larger radius c .

2. Theoretical description

2.1. Field equation and characteristic equations

A shielded composite dielectric spherical shell resonator with a metallic sphere studied presently is shown in Fig. 1. A perfectly conducting metallic sphere of radius a is concentrically surrounded by a dielectric sphere of radius b and permittivity ϵ_1 which in turn is surrounded by another concentric dielectric sphere of radius c and permittivity ϵ_2 . The whole assembly is shielded by a perfectly conducting concentric spherical metal case of radius c . The materials of the two dielectric spheres are non-magnetic, i.e. $\mu_1 = \mu_0 = \mu_2$. Now the resonator consists of two regions, one in the region $a \leq r \leq b$ and the other in the region $b \leq r \leq c$.

The solution of the radial part of the wave equation in the two dielectric spheres [8–26,36–41] is given by

$$X(r) = A_j J_{n+\frac{1}{2}}(k_j r) + B_j Y_{n+\frac{1}{2}}(k_j r) \quad (1)$$

with $j=1$ for region $a < r < b$ and $j=2$ for region $b < r < c$ where, $(\sqrt{\omega^2 \mu_0 \epsilon_0 \epsilon_1})r = (\omega \sqrt{\mu_0 \epsilon_0 \epsilon_1})r = (\frac{\omega}{c} \sqrt{\epsilon_1})r = kr$, k is the wave number, $c = \frac{1}{\sqrt{\mu_0 \epsilon_0}}$ is the speed of light in vacuum, $k_1 = \frac{\omega}{c} \sqrt{\epsilon_1} = k_0 \sqrt{\epsilon_1}$ and $k_2 = \frac{\omega}{c} \sqrt{\epsilon_2} = k_0 \sqrt{\epsilon_2}$ where $c = \frac{1}{\sqrt{\mu_0 \epsilon_0}}$ is the speed of light in vacuum, $P_n^m(\cos \theta)$ [Appendix-B, Eqs. (B10) and (B11)] is called associated Legendre polynomial of the first kind, $J_{n+\frac{1}{2}}(kr)$ and $Y_{n+\frac{1}{2}}(kr)$ are the Bessel function of the first kind and second kind of order $(n + \frac{1}{2})$ respectively. Since, $Y_{n+\frac{1}{2}}(kr)$ (Appendix-C) has infinite value at $r=0$, any linear combination of $J_{n+\frac{1}{2}}(kr)$ and $Y_{n+\frac{1}{2}}(kr)$ also has finite value at $r=0$. But at $r=0$ the field vectors have finite values, and A_j and B_j are constants and ϵ_{r1} and ϵ_{r2} are the dielectric constants of the inner and outer dielectric spheres. Therefore, excepting a normalization constant for the product of $P_n^m(\cos \theta)$ and $\cos m \phi$, the solutions of the wave-equations in the two regions [1–8, 36–41] are given by,

$$\psi(r, \theta, \phi) = \{A_j J_{n+\frac{1}{2}}(k_j r) + B_j Y_{n+\frac{1}{2}}(k_j r)\} P_n^m(\cos \theta) \cos m \phi \quad (2)$$

where $j=1$ for region $a < r < b$ and $j=2$ for region $b < r < c$ (Appendix-A1).

This expression for $\psi(r, \theta, \phi)$ from Eq. (2) one can be used to find out the expressions for the field components for the $TE_{nm\ell}$ and the $TM_{nm\ell}$ modes separately [1–8,36–40].

Following the procedures adopted in earlier [38–41] the field expression for the $TE_{nm\ell}$ and the $TM_{nm\ell}$ modes have been determined and are collected in Sections 2.1.1 and 2.1.2.

2.1.1. Field expressions for the $TE_{nm\ell}$ modes

$$\left. \begin{aligned} E_r &= 0 \\ E_\theta &= \frac{-i\omega\mu_0}{\sqrt{k_j r}} \frac{m}{\sin\theta} \{A_j J_{n+\frac{1}{2}}(k_j r) + B_j Y_{n+\frac{1}{2}}(k_j r)\} P_n^m(\cos\theta) \frac{d}{d\phi} (e^{im\phi}) \\ E_\phi &= \frac{i\omega\mu_0}{\sqrt{k_j r}} \{A_j J_{n+\frac{1}{2}}(k_j r) + B_j Y_{n+\frac{1}{2}}(k_j r)\} \frac{d}{d\theta} \{P_n^m(\cos\theta)\} e^{im\phi} \\ H_r &= \frac{n(n+1)}{r\sqrt{k_j r}} \{A_j J_{n+\frac{1}{2}}(k_j r) + B_j Y_{n+\frac{1}{2}}(k_j r)\} P_n^m(\cos\theta) e^{im\phi} \\ H_\theta &= \frac{1}{r\sqrt{k_j}} \frac{d}{dr} \sqrt{r} \{A_j J_{n+\frac{1}{2}}(k_j r) + B_j Y_{n+\frac{1}{2}}(k_j r)\} \frac{d}{d\theta} \{P_n^m(\cos\theta)\} e^{im\phi} \\ H_\phi &= \frac{m}{r\sqrt{k_j \sin\theta}} \frac{d}{dr} \sqrt{r} \{A_j J_{n+\frac{1}{2}}(k_j r) + B_j Y_{n+\frac{1}{2}}(k_j r)\} P_n^m(\cos\theta) \frac{d}{d\phi} (e^{im\phi}) \end{aligned} \right\} \quad (3)$$

where $i = \sqrt{-1}$, $j=1$ for inner dielectric spherical region ($a < r < b$) and $j=2$ for dielectric spherical region ($b < r < c$).

2.1.2. Field expression for the $TE_{nm\ell}$ modes

$$\left. \begin{aligned} E_r &= \frac{n(n+1)}{r\sqrt{k_j r}} \{A_j J_{n+\frac{1}{2}}(k_j r) + B_j Y_{n+\frac{1}{2}}(k_j r)\} P_n^m(\cos\theta) e^{im\phi} \\ E_\theta &= \frac{1}{r\sqrt{k_j}} \frac{d}{dr} \sqrt{r} \{A_j J_{n+\frac{1}{2}}(k_j r) + B_j Y_{n+\frac{1}{2}}(k_j r)\} \frac{d}{d\theta} \{P_n^m(\cos\theta)\} e^{im\phi} \\ E_\phi &= \frac{1}{r\sqrt{k_j}} \frac{m}{\sin\theta} \frac{d}{dr} \sqrt{r} \{A_j J_{n+\frac{1}{2}}(k_j r) + B_j Y_{n+\frac{1}{2}}(k_j r)\} P_n^m(\cos\theta) \frac{d}{d\phi} (e^{im\phi}) \\ H_r &= 0 \\ H_\theta &= \frac{i\omega\epsilon_0 \epsilon_j^r m}{\sqrt{k_j r \sin\theta}} \{A_j J_{n+\frac{1}{2}}(k_j r) + B_j Y_{n+\frac{1}{2}}(k_j r)\} P_n^m(\cos\theta) \frac{d}{d\phi} (e^{im\phi}) \\ H_\phi &= -\frac{i\omega\epsilon_0 \epsilon_j^r}{\sqrt{k_j r}} \{A_j J_{n+\frac{1}{2}}(k_j r) + B_j Y_{n+\frac{1}{2}}(k_j r)\} \frac{d}{d\theta} \{P_n^m(\cos\theta)\} e^{im\phi} \end{aligned} \right\} \quad (4)$$

where $j=1$ for inner dielectric spherical region ($a < r < b$) and $j=2$ for dielectric spherical region ($b < r < c$).

In order to derive the characteristic equations for the $TE_{nm\ell}$ modes boundary conditions that the tangential components of \vec{E} (E_θ and E_ϕ) must vanish for all θ and ϕ on metal surfaces i.e. at $r=a$ and $r=c$, and the tangential components of \vec{E} and \vec{H} are continuous at $r=b$ are used. Applying these conditions one gets from Eq. (3) the following relations,

$$W_{TE} V = 0 \quad (5)$$

where

$$W_{TE} = \begin{pmatrix} J_{n+\frac{1}{2}}(k_1 a) & Y_{n+\frac{1}{2}}(k_1 a) & 0 & 0 \\ 0 & 0 & J_{n+\frac{1}{2}}(k_2 c) & Y_{n+\frac{1}{2}}(k_2 c) \\ \frac{1}{\sqrt{k_1}} J_{n+\frac{1}{2}}(k_1 b) & \frac{1}{\sqrt{k_1}} Y_{n+\frac{1}{2}}(k_1 b) & -\frac{1}{\sqrt{k_2}} J_{n+\frac{1}{2}}(k_2 b) & -\frac{1}{\sqrt{k_2}} Y_{n+\frac{1}{2}}(k_2 b) \\ \frac{1}{\sqrt{k_1}} J_{n+\frac{1}{2}}(k_1 b) & \frac{1}{\sqrt{k_1}} Y_{n+\frac{1}{2}}(k_1 b) & -\frac{1}{\sqrt{k_2}} \{J_{n+\frac{1}{2}}(k_2 b) & -\frac{1}{\sqrt{k_2}} \{J_{n+\frac{1}{2}}(k_2 b) \\ +2bk_1 J'_{n+\frac{1}{2}}(k_1 b) & +2bk_1 Y'_{n+\frac{1}{2}}(k_1 b) & +2bk_2 J'_{n+\frac{1}{2}}(k_2 b) & +2bk_2 J'_{n+\frac{1}{2}}(k_2 b)\} \end{pmatrix} \quad (6)$$

and

$$V = (A_1, B_1, A_2, B_2)^T \quad (7)$$

In order to satisfy Eq. (5) simultaneously determinant of the coefficients must vanish, i.e.

$$\det W_{TE} = 0 \quad (8)$$

Eq. (8) represents the characteristic equation for the $TE_{nm\ell}$ modes and on simplification it reduces to,

$$\begin{aligned} & Y_{n+\frac{1}{2}}(k_1 a) \bar{J}_{n+\frac{1}{2}}(k_1 b) \{J_{n+\frac{1}{2}}(k_2 b) Y_{n+\frac{1}{2}}(k_2 c) - J_{n+\frac{1}{2}}(k_2 c) Y_{n+\frac{1}{2}}(k_2 b)\} \\ & + J_{n+\frac{1}{2}}(k_1 a) \bar{Y}_{n+\frac{1}{2}}(k_1 b) \{J_{n+\frac{1}{2}}(k_2 c) Y_{n+\frac{1}{2}}(k_2 b) - J_{n+\frac{1}{2}}(k_2 b) Y_{n+\frac{1}{2}}(k_2 c)\} \\ & + J_{n+\frac{1}{2}}(k_1 b) Y_{n+\frac{1}{2}}(k_1 a) \{J_{n+\frac{1}{2}}(k_2 c) \bar{Y}_{n+\frac{1}{2}}(k_2 b) - Y_{n+\frac{1}{2}}(k_2 c) \bar{J}_{n+\frac{1}{2}}(k_2 b)\} \\ & + J_{n+\frac{1}{2}}(k_1 a) Y_{n+\frac{1}{2}}(k_1 b) \{Y_{n+\frac{1}{2}}(k_2 c) \bar{J}_{n+\frac{1}{2}}(k_2 b) - J_{n+\frac{1}{2}}(k_2 c) \bar{Y}_{n+\frac{1}{2}}(k_2 b)\} = 0 \end{aligned} \quad (9)$$

where

$$\begin{aligned} \bar{J}_{n+\frac{1}{2}}(k_1 b) &= J_{n+\frac{1}{2}}(k_1 b) + 2bk_1 J'_{n+\frac{1}{2}}(k_1 b) \\ \bar{J}_{n+\frac{1}{2}}(k_2 b) &= J_{n+\frac{1}{2}}(k_2 b) + 2bk_2 J'_{n+\frac{1}{2}}(k_2 b) \\ \bar{Y}_{n+\frac{1}{2}}(k_1 b) &= Y_{n+\frac{1}{2}}(k_1 b) + 2bk_1 Y'_{n+\frac{1}{2}}(k_1 b) \\ \bar{Y}_{n+\frac{1}{2}}(k_2 b) &= Y_{n+\frac{1}{2}}(k_2 b) + 2bk_2 Y'_{n+\frac{1}{2}}(k_2 b) \end{aligned} \quad (10)$$

Similarly, applying the boundary conditions at $r=a$, $r=b$ and $r=c$ and using Eq. (4) one has,

$$W'_{TE} V = 0 \quad (11)$$

where,

$$W'_{TE} = \begin{pmatrix} J_{n+\frac{1}{2}}(k_1a) & Y_{n+\frac{1}{2}}(k_1a) & 0 & 0 \\ +2ak_1J'_{n+\frac{1}{2}}(k_1a) & +2ak_1Y'_{n+\frac{1}{2}}(k_1a) & 0 & 0 \\ 0 & 0 & J_{n+\frac{1}{2}}(k_2c) & Y_{n+\frac{1}{2}}(k_2c) \\ \frac{\epsilon_r}{\sqrt{k_1}}J_{n+\frac{1}{2}}(k_1b) & \frac{\epsilon_r}{\sqrt{k_1}}Y_{n+\frac{1}{2}}(k_1b) & -\frac{\epsilon_s}{\sqrt{k_2}}J_{n+\frac{1}{2}}(k_2b) & -\frac{\epsilon_s}{\sqrt{k_2}}Y_{n+\frac{1}{2}}(k_2b) \\ \frac{1}{\sqrt{k_1}}\{J_{n+\frac{1}{2}}(k_1b)\} & \frac{1}{\sqrt{k_1}}\{Y_{n+\frac{1}{2}}(k_1b)\} & -\frac{1}{\sqrt{k_2}}\{J_{n+\frac{1}{2}}(k_2b)\} & -\frac{1}{\sqrt{k_2}}\{Y_{n+\frac{1}{2}}(k_2b)\} \\ +2bk_1J'_{n+\frac{1}{2}}(k_1b) & +2bk_1Y'_{n+\frac{1}{2}}(k_1b) & +2k_2bJ'_{n+\frac{1}{2}}(k_2b) & +2k_2bY'_{n+\frac{1}{2}}(k_2b) \end{pmatrix} \tag{12}$$

And

$$V = (A_1, B_1, A_2, B_2)^T \tag{13}$$

From Eq. (11) we get the determinantal form of the characteristic equation for the $TM_{nm\ell}$ modes as,

$$\det W'_{TE} = 0 \tag{14}$$

After simplification Eq. (14) has the following form:

$$\begin{aligned} & \bar{Y}_{n+\frac{1}{2}}(k_1a)Y_{n+\frac{1}{2}}(k_2c) \left\{ \epsilon_2^r J_{n+\frac{1}{2}}(k_2b)\bar{J}_{n+\frac{1}{2}}(k_1b) - \epsilon_1^r J_{n+\frac{1}{2}}(k_1b)\bar{J}_{n+\frac{1}{2}}(k_2b) \right\} \\ & + \bar{J}_{n+\frac{1}{2}}(k_1a)\bar{J}_{n+\frac{1}{2}}(k_2c) \left\{ \epsilon_2^r Y_{n+\frac{1}{2}}(k_2b)\bar{Y}_{n+\frac{1}{2}}(k_1b) - \epsilon_1^r Y_{n+\frac{1}{2}}(k_1b)\bar{Y}_{n+\frac{1}{2}}(k_2b) \right\} \\ & + \bar{J}_{n+\frac{1}{2}}(k_1a)\bar{Y}_{n+\frac{1}{2}}(k_2c) \left\{ \epsilon_1^r Y_{n+\frac{1}{2}}(k_1b)\bar{J}_{n+\frac{1}{2}}(k_2b) - \epsilon_2^r J_{n+\frac{1}{2}}(k_2b)\bar{Y}_{n+\frac{1}{2}}(k_1b) \right\} \\ & + \bar{J}_{n+\frac{1}{2}}(k_2c)\bar{Y}_{n+\frac{1}{2}}(k_1a) \left\{ \epsilon_1^r J_{n+\frac{1}{2}}(k_1b)\bar{Y}_{n+\frac{1}{2}}(k_2b) - \epsilon_2^r Y_{n+\frac{1}{2}}(k_2b)\bar{J}_{n+\frac{1}{2}}(k_1b) \right\} = 0 \end{aligned} \tag{15}$$

where

$$\begin{aligned} \bar{J}_{n+\frac{1}{2}}(k_1a) &= J_{n+\frac{1}{2}}(k_1a) + 2ak_1J'_{n+\frac{1}{2}}(k_1a) \\ \bar{J}_{n+\frac{1}{2}}(k_2c) &= J_{n+\frac{1}{2}}(k_2c) + 2ck_2J'_{n+\frac{1}{2}}(k_2c) \\ \bar{Y}_{n+\frac{1}{2}}(k_1a) &= Y_{n+\frac{1}{2}}(k_1a) + 2ak_1Y'_{n+\frac{1}{2}}(k_1a) \\ \bar{Y}_{n+\frac{1}{2}}(k_2c) &= Y_{n+\frac{1}{2}}(k_2c) + 2ck_2Y'_{n+\frac{1}{2}}(k_2c) \end{aligned} \tag{16}$$

2.2. Energy, losses and quality factors

2.2.1. Energy

The energy W stored in the dielectric sphere is given by [22,23,41],

$$W = \frac{1}{2} \epsilon \iiint_V \vec{E} \cdot \vec{E}^* dV = \frac{1}{2} \mu \iiint_V \vec{H} \cdot \vec{H}^* dV \tag{17}$$

Here W is the sum of the energies W_1 , stored in the inner dielectric sphere $a \leq r \leq b$ and W_2 , stored in the outer dielectric sphere $b \leq r \leq c$.

For the $TE_{nm\ell}$ modes

$$W_{j,n}^{TE} = \frac{1}{2} \epsilon_0 \epsilon_j^r \int_0^{2\pi} \int_0^\pi \int_a^b \vec{E} \cdot \vec{E}^* r^2 \sin\theta \, dr \, d\theta \, d\phi \tag{18}$$

Where, the value of index j changes from 1 to 2.

For the $TE_{10\ell}$ modes

$$\left. \begin{aligned} E_r &= 0 \\ E_\theta &= 0 \end{aligned} \right\} \tag{19}$$

$$\begin{aligned} E_\phi &= -\frac{i\omega\mu_0}{\sqrt{k_j r}} \{A_j J_{3/2}(k_j r) + B_j Y_{3/2}(k_j r)\} \sin\theta \\ E_\phi \cdot E_\phi^* &= \frac{\omega^2 \mu_0^2}{k_j r} \{A_j J_{3/2}(k_j r) + B_j Y_{3/2}(k_j r)\}^2 \sin^2\theta \end{aligned} \tag{20}$$

where index $j = 1$ for $TE_{10\ell}$ modes in the region $a < r < b$ and index $j = 2$ for $TE_{10\ell}$ modes in the region $b < r < c$.

From Eqs. (18) and (19) one gets for the region $a < r < b$ as,

$$W_{1,1}^{TE} = \frac{4\pi\omega^2\mu_0^2\epsilon_0}{3k_1} \int_a^b r \{A_1 J_{3/2}(k_1 r) + B_1 Y_{3/2}(k_1 r)\}^2 \, dr \tag{21}$$

Using the results of integrals involving Bessel's functions Eq. (21) gives,

$$\begin{aligned} W_{1,1}^{TE} &= \omega^2 \mu_0^2 \epsilon_0 \epsilon_1^r [A_1^2 r^3 \{j_1^2(k_1 r) - j_0(k_1 r) j_2(k_1 r)\} + B_1^2 r^3 \{y_1^2(k_1 r) - y_0(k_1 r) y_2(k_1 r)\} \\ &+ A_1 B_1 r^2 \{2y_1(k_1 r) j_1(k_1 r) - y_0(k_1 r) j_2(k_1 r) - y_2(k_1 r) j_0(k_1 r)\}]_a^b \end{aligned} \tag{22}$$

From Eqs. (19) and (20) one gets for the region $b < r < c$ as,

$$W_{2,1}^{TE} = \frac{4\pi \omega^2 \mu_0^2 \epsilon_0 \epsilon_2^r}{3k_2} \int_b^c r \{A_2 J_{3/2}(k_2 r) + B_2 Y_{3/2}(k_2 r)\}^2 dr \tag{23}$$

which on further simplification reduces to,

$$W_{2,1}^{TE} = \frac{4}{3} \omega^2 \mu_0^2 \epsilon_0 \epsilon_2^r [A_2^2 r^3 \{j_1^2(k_2 r) - j_0(k_2 r)j_2(k_2 r)\} + B_2^2 r^3 \{y_1^2(k_2 r) - y_0(k_2 r)y_2(k_2 r)\} + A_2 B_2 r^3 \{2y_1(k_2 r)j_1(k_2 r) - y_0(k_2 r)j_2(k_2 r) - y_2(k_2 r)j_0(k_2 r)\}]_b^c \tag{24}$$

The expressions of energy stored in the dielectric spheres for the $TE_{20\ell}$ and $TE_{30\ell}$ modes are determined similarly and are given as,

$$W_{1,2}^{TE} = \frac{12}{5} \omega^2 \mu_0^2 \epsilon_0 \epsilon_1^r [A_1^2 r^3 \{j_2^2(k_1 r) - j_1(k_1 r)j_3(k_1 r)\} + B_1^2 r^3 \{y_2^2(k_1 r) - y_1(k_1 r)y_3(k_1 r)\} + A_1 B_1 r^3 \{2y_2(k_1 r)j_2(k_1 r) - y_1(k_1 r)j_3(k_1 r) - y_3(k_1 r)j_1(k_1 r)\}]_a^b \tag{25}$$

$$W_{2,2}^{TE} = \frac{12}{5} \omega^2 \mu_0^2 \epsilon_0 \epsilon_2^r [A_2^2 r^3 \{j_2^2(k_2 r) - j_1(k_2 r)j_3(k_2 r)\} + B_2^2 r^3 \{y_2^2(k_2 r) - y_1(k_2 r)y_3(k_2 r)\} + A_2 B_2 r^3 \{2y_2(k_2 r)j_2(k_2 r) - y_1(k_2 r)j_3(k_2 r) - y_3(k_2 r)j_1(k_2 r)\}]_b^c \tag{26}$$

$$W_{1,3}^{TE} = \frac{24}{7} \omega^2 \mu_0^2 \epsilon_0 \epsilon_1^r [A_1^2 r^3 \{j_3^2(k_1 r) - j_2(k_1 r)j_4(k_1 r)\} + B_1^2 r^3 \{y_3^2(k_1 r) - y_2(k_1 r)y_4(k_1 r)\} + A_1 B_1 \{2y_3(k_1 r)j_3(k_1 r) - y_2(k_1 r)j_4(k_1 r) - y_4(k_1 r)j_2(k_1 r)\}]_a^b \tag{27}$$

$$W_{2,3}^{TE} = \frac{24}{7} \omega^2 \mu_0^2 \epsilon_0 \epsilon_2^r [A_2^2 r^3 \{j_3^2(k_2 r) - j_2(k_2 r)j_4(k_2 r)\} + B_2^2 r^3 \{y_3^2(k_2 r) - y_2(k_2 r)y_4(k_2 r)\} + A_2 B_2 \{2y_3(k_2 r)j_3(k_2 r) - y_2(k_2 r)j_4(k_2 r) - y_4(k_2 r)j_2(k_2 r)\}]_b^c \tag{28}$$

where B_1 , A_2 and B_2 used for the $TE_{nm\ell}$ modes Eqs. (22), ((25)–(28)) are determined in terms of A_1 using Eqs. (5)–(7) as,

$$B_1 = -\frac{j_n(k_1 a)}{y_n(k_1 a)} A_1 \tag{29}$$

$$A_2 = -\frac{\epsilon_2^r y_n(k_2 c) \{j_n(k_1 b) y_n(k_1 a) - j_n(k_1 a) y_n(k_1 b)\}}{\epsilon_1^r y_n(k_1 a) \{y_n(k_2 b) j_n(k_2 c) - j_n(k_2 b) y_n(k_2 c)\}} A_1 \tag{30}$$

$$B_2 = \frac{\epsilon_2^r j_n(k_2 c) \{j_n(k_1 b) y_n(k_1 a) - j_n(k_1 a) y_n(k_1 b)\}}{\epsilon_1^r y_n(k_1 a) \{y_n(k_2 b) j_n(k_2 c) - j_n(k_2 b) y_n(k_2 c)\}} A_1 \tag{31}$$

Similarly, the expressions for energy $W_{j,n}^{TM}$ stored in the dielectric spheres for the $TM_{nm\ell}$ modes are determined as follows,

$$W_{1,n}^{TM} = \frac{1}{2} \mu_0 \int_0^{2\pi} \int_0^\pi \int_a^b \vec{H} \cdot \vec{H}^* r^2 \sin\theta \, dr \, d\theta \, d\phi \tag{32}$$

$$W_{2,n}^{TM} = \frac{1}{2} \mu_0 \int_0^{2\pi} \int_0^\pi \int_b^c \vec{H} \cdot \vec{H}^* r^2 \sin\theta \, dr \, d\theta \, d\phi \tag{33}$$

For the $TM_{10\ell}$ modes

$$\left. \begin{aligned} H_r &= 0 \\ H_\theta &= 0 \\ H_\phi &= \frac{i\omega\epsilon_0\epsilon_j^r}{\sqrt{k_j r}} \{A_j J_{3/2}(k_j r) + B_j Y_{3/2}(k_j r)\} \sin\theta \\ H_\phi \cdot H_\phi^* &= \frac{\omega^2 \epsilon_0^2 (\epsilon_j^r)^2}{k_j r} \{A_j J_{3/2}(k_j r) + B_j Y_{3/2}(k_j r)\}^2 \sin^2\theta \end{aligned} \right\} \tag{34}$$

where index $j=1$ for $TM_{10\ell}$ modes in the region $a < r < b$ and index $j=2$ for $TM_{10\ell}$ modes in the region $b < r < c$.

From Eqs. (32) and (34) one gets for $j=1$ in the region $a < r < b$ as,

$$W_{1,1}^{TM} = \frac{4\pi \omega^2 \mu_0 \epsilon_0^2 (\epsilon_1^r)^2}{3k_1} \int_a^b r \{A_1 J_{3/2}(k_1 r) + B_1 Y_{3/2}(k_1 r)\}^2 dr \tag{35}$$

which becomes,

$$W_{1,1}^{TM} = \frac{4}{3} \omega^2 \mu_0 \epsilon_0^2 (\epsilon_1^r)^2 [A_1^2 r^3 \{j_1^2(k_1 r) - j_0(k_1 r)j_2(k_1 r)\} + B_1^2 r^3 \{y_1^2(k_1 r) - y_0(k_1 r)y_2(k_1 r)\} + A_1 B_1 r^3 \{2j_1(k_1 r)y_1(k_1 r) - y_0(k_1 r)j_2(k_1 r) - y_2(k_1 r)j_0(k_1 r)\}]_a^b \tag{36}$$

Hence, using Eqs. (33) and (34) one gets for $j=2$ in the region $b < r < c$ as,

$$W_{2,1}^{TM} = \frac{4\pi \omega^2 \mu_0 \epsilon_0^2 (\epsilon_2^r)^2}{3k_2} \int_b^c r \{A_2 J_{3/2}(k_2 r) + B_2 Y_{3/2}(k_2 r)\}^2 dr \tag{37}$$

The above equation is simplified to,

$$W_{2,1}^{TM} = \frac{4}{3} \omega^2 \mu_0 \epsilon_0^2 (\epsilon_2^r)^2 [A_2^2 r^3 \{j_1^2(k_2 r) - j_0(k_2 r)j_2(k_2 r)\} + B_2^2 r^3 \{y_1^2(k_2 r) - y_0(k_2 r)y_1(k_2 r) - y_0(k_2 r)j_2(k_2 r) - y_2(k_2 r)j_0(k_2 r)\}]_c^d \tag{38}$$

The expressions for energy stored in $TM_{20\ell}$ and $TM_{30\ell}$ modes are determined by similar procedure and these are given below:

$$W_{1,2}^{TM} = \frac{12}{5} \omega^2 \mu_0 \epsilon_0^2 (\epsilon_1^r)^2 [A_1^2 r^3 \{j_2^2(k_1 r) - j_1(k_1 r)j_3(k_1 r)\} + B_1^2 r^3 \{y_2^2(k_1 r) - y_1(k_1 r)y_3(k_1 r)\} + A_1 B_1 r^3 \{2y_2(k_1 r)j_2(k_1 r) - y_1(k_1 r)j_3(k_1 r) - y_3(k_1 r)j_1(k_1 r)\}]_a^b \tag{39}$$

$$W_{2,2}^{TM} = \frac{12}{5} \omega^2 \mu_0 \epsilon_0^2 (\epsilon_2^r)^2 [A_2^2 r^3 \{j_2^2(k_2 r) - j_1(k_2 r)j_3(k_2 r)\} + B_2^2 r^3 \{y_2^2(k_2 r) - y_1(k_2 r)y_3(k_2 r)\} + A_1 B_1 r^3 \{2y_2(k_2 r)j_2(k_2 r) - y_1(k_2 r)j_3(k_2 r) - y_3(k_2 r)j_1(k_2 r)\}]_b^c \tag{40}$$

$$W_{1,3}^{TM} = \frac{24}{7} \omega^2 \mu_0 \epsilon_0^2 (\epsilon_1^r)^2 [A_1^2 r^3 \{j_3^2(k_1 r) - j_2(k_1 r)j_4(k_1 r)\} + B_1^2 r^3 \{y_3^2(k_1 r) - y_2(k_1 r)y_4(k_1 r)\} + A_1 B_1 r^3 \{2y_3(k_1 r)j_3(k_1 r) - y_2(k_1 r)j_4(k_1 r) - y_4(k_1 r)j_2(k_1 r)\}]_a^b \tag{41}$$

$$W_{2,3}^{TM} = \frac{24}{7} \omega^2 \mu_0 \epsilon_0^2 (\epsilon_2^r)^2 [A_1^2 r^3 \{j_3^2(k_2 r) - j_2(k_2 r)j_4(k_2 r)\} + B_1^2 r^3 \{y_3^2(k_2 r) - y_2(k_2 r)y_4(k_2 r)\} + A_1 B_1 r^3 \{2y_3(k_2 r)j_3(k_2 r) - y_2(k_2 r)j_4(k_2 r) - y_4(k_2 r)j_2(k_2 r)\}]_b^c \tag{42}$$

where the constants B_1, A_2 and B_2 used for the $TM_{nm\ell}$ modes (Eqs. 41, 44-48) are determined in terms of A_1 using Eqs. (14) as,

$$B_1 = - \frac{y_n(k_1 a) + a k_1 y'_n(k_1 a)}{j_n(k_1 a) + a k_1 j'_n(k_1 a)} A_1 \tag{43}$$

$$A_2 = - \frac{\epsilon_1^r \{y_n(k_2 c) + k_2 c y'_n(k_2 c)\} [j_n(k_1 b) \{j_n(k_1 a) + k_1 a j'_n(k_1 a)\} - y_n(k_1 b) \{y_n(k_1 a) + k_1 a y'_n(k_1 a)\}]}{\epsilon_2^r \{j_n(k_1 a) + k_1 a j'_n(k_1 a)\} [j_n(k_2 b) \{y_n(k_2 c) + k_2 c y'_n(k_2 c)\} - y_n(k_2 b) \{j_n(k_2 c) + k_2 c j'_n(k_2 c)\}]} A_1 \tag{44}$$

$$B_2 = \frac{\epsilon_1^r \{j_n(k_2 c) + k_2 c j'_n(k_2 c)\} [j_n(k_1 b) \{j_n(k_1 a) + k_1 a j'_n(k_1 a)\} - y_n(k_1 b) \{y_n(k_1 a) + k_1 a y'_n(k_1 a)\}]}{\epsilon_2^r \{j_n(k_1 a) + k_1 a j'_n(k_1 a)\} [j_n(k_2 b) \{y_n(k_2 c) + k_2 c y'_n(k_2 c)\} - y_n(k_2 b) \{j_n(k_2 c) + k_2 c j'_n(k_2 c)\}]} A_1 \tag{45}$$

where j'_n and y'_n are first derivatives of j_n and y_n respectively [1-15,38-41].

2.3. Losses

Here the power loss P of the system is given by,

$$P = P_m + P_d \tag{46}$$

where P_m is the sum of metallic losses on the inner and the outer metal sphere surfaces and P_d is the sum of the dielectric losses due to finite conductivities of the dielectric spheres [1-15,36-41].

The metal loss is calculated assuming that the inner metal sphere and the shield are of same material [1-15].

$$P_m = \frac{1}{2} R_s \iint_{\text{metallic surfaces } (r=a,c)} \vec{H} \cdot \vec{H}^* dS \tag{47}$$

The loss P_d in the dielectric spheres is calculated by,

$$P_d = \frac{1}{2} \sigma_d \iiint_{\text{dielectric volume}} \vec{E} \cdot \vec{E}^* dV \tag{48}$$

where right hand side of Eq. (48) is evaluated for the two spheres (dielectric) separately [1-8,36-41].

2.3.1. Metallic losses for the TE modes

For the $TE_{10\ell}$ mode

$$\left. \begin{aligned} H_r &= 0 \\ H_\phi &= 0 \\ H_\theta &= -\frac{1}{r\sqrt{k_1}} \frac{d}{dr} \left\{ \sqrt{r} (A_j j_{3/2}(k_j r) + B_j Y_{3/2}(k_j r)) \right\} \sin\theta \\ H_\theta \cdot H_\theta^* &= \frac{2k_1^2}{\pi} \left\{ A_j j'_1(k_j r) + B_j y'_1(k_j r) \right\}^2 \sin^2\theta \end{aligned} \right\} \tag{49}$$

where index $j=1$ for $TE_{10\ell}$ modes in the region $a < r < b$ and index $j=2$ for $TE_{10\ell}$ modes in the region $b < r < c$.

Using Eqs. (47) and (49) we get metallic loss on spherical metal surface $r=a$ for $j=1$ in the region $a < r < b$ as,

$$P_{m,1}^a = \frac{R_s k_1^2}{\pi} \iint_{r=a} \{A_{1j'_1}(k_1 r) + B_{1y'_1}(k_1 r)\}^2 r^2 \sin^3 \theta \, d\theta \, d\phi \tag{50}$$

which is simplified to,

$$P_{m,1}^a = \frac{8}{3} \sqrt{\frac{\omega \mu_0}{2\sigma}} k_1^2 a^2 \{A_{1j'_1}(k_1 a) + B_{1y'_1}(k_1 a)\}^2 \tag{51}$$

Using Eqs. (47) and (51) we get metallic loss on spherical metal surface $r=c$, for $j=2$ in the region $b < r < c$ as,

$$P_{m,1}^c = \frac{R_s k_2^2}{\pi} \iint_{r=c} \{A_{2j'_1}(k_2 r) + B_{2y'_1}(k_2 r)\}^2 r^2 \sin^3 \theta \, d\theta \, d\phi \tag{52}$$

or

$$P_{m,1}^c = \frac{8}{3} \sqrt{\frac{\omega \mu_0}{2\sigma}} k_2^2 c^2 \{A_{2j'_1}(k_2 c) + B_{2y'_1}(k_2 c)\} \tag{53}$$

Thus, the total metallic loss on surfaces $r=a$ and $r=c$ is obtained by adding the RHS of Eqs. (50) and (53) as,

$$P_{m,1} = \frac{8}{3} \sqrt{\frac{\omega \mu_0}{2\sigma}} \left\{ k_1^2 a^2 (A_{1j'_1}(k_1 a) + B_{1y'_1}(k_1 a))^2 + k_2^2 c^2 (A_{2j'_1}(k_2 c) + B_{2y'_1}(k_2 c))^2 \right\} \tag{54}$$

Similarly, the expressions of the metallic loss on surface $r=a$ and $r=c$ for the $TE_{20\ell}$ and $TE_{30\ell}$ modes are given by,

$$P_{m,2} = \frac{24}{5} \sqrt{\frac{\omega \mu_0}{2\sigma}} \left\{ k_1^2 a^2 (A_{j'_2}(k_1 a) + B_{y'_2}(k_1 a))^2 + k_2^2 c^2 (C_{j'_2}(k_2 c) + D_{y'_2}(k_2 c))^2 \right\} \tag{55}$$

$$P_{m,3} = \frac{48}{7} \sqrt{\frac{\omega \mu_0}{2\sigma}} \left\{ k_1^2 a^2 (A_{1j'_3}(k_1 a) + B_{1y'_3}(k_1 a))^2 + k_2^2 c^2 (A_{2j'_3}(k_2 c) + B_{2y'_3}(k_2 c))^2 \right\} \tag{56}$$

2.3.2. Dielectric losses for the TE modes

Dielectric loss for the $TE_{10\ell}$, $TE_{20\ell}$ and $TE_{30\ell}$ modes are calculated to be,

$$P_{d,1} = \omega (W_{1,1}^{TE} + W_{2,1}^{TE}) \tan \delta \tag{57}$$

$$P_{d,2} = \omega (W_{1,2}^{TE} + W_{2,2}^{TE}) \tan \delta \tag{58}$$

$$P_{d,3} = \omega (W_{1,3}^{TE} + W_{2,3}^{TE}) \tan \delta \tag{59}$$

Where, $\tan \delta$ represents the loss tangent for a dielectric material, which is defined by $\tan \delta = \sigma / (\omega \epsilon_0 \epsilon_r)$ where ϵ_r is the dielectric constant of the medium and ϵ_0 is the permittivity of vacuum, σ is conductivity of the medium, and ω is frequency [1-8,41]

2.3.3. Metallic losses for the TM modes

For the $TM_{10\ell}$ mode

$$\left. \begin{aligned} H_r &= 0 \\ H_\theta &= 0 \\ H_\phi &= \frac{i\omega \epsilon_0 \epsilon_r^i}{\sqrt{k_j r}} \{A_{1j_{3/2}}(k_j r) + B_{j_{3/2}}(k_j r)\} \sin \theta \\ H_\phi \cdot H_\phi^* &= \frac{\omega^2 \epsilon_0^2 (\epsilon_r^i)^2}{k_j r} \{A_{j_{3/2}}(k_j r) + B_{j_{3/2}}(k_j r)\}^2 \sin^2 \theta \end{aligned} \right\} \tag{60}$$

where index $j=1$ for $TM_{10\ell}$ modes in the region $a < r < b$ and index $j=2$ for $TM_{10\ell}$ modes in the region $b < r < c$.

Using Eqs. (47) and (60) for the region $a < r < b$ one gets,

$$P_{m,1}^a = \frac{\omega^2 \epsilon_0 (\epsilon_r^i)^2}{\pi} R_s \iint_{r=a} \{A_{j_1}(k_1 r) + B_{y_1}(k_1 r)\}^2 r^2 \sin^3 \theta \, d\theta \, d\phi \tag{61}$$

or

$$P_{m,1}^a = \frac{8}{3} \sqrt{\frac{\omega \mu_0}{2\sigma}} \omega^2 \epsilon_0^2 (\epsilon_r^i)^2 a^2 \{A_{1j_1}(k_1 a) + B_{1y_1}(k_1 a)\}^2 \tag{62}$$

Using Eq. (47) and (62) we get the metallic loss on $r=c$ for index $j=2$ in the region $b < r < c$ as,

$$P_{m,1}^c = \frac{\omega^2 \epsilon_0^2 (\epsilon_r^i)^2}{\pi} R_s \iint_{r=c} \{A_{2j_1}(k_2 r) + B_{2y_1}(k_2 r)\}^2 r^2 \sin^3 \theta \, d\theta \, d\phi \tag{63}$$

which is simplified to,

$$P_{m,1}^c = \frac{8}{3} \sqrt{\frac{\omega \mu_0}{2\sigma}} \omega^2 \epsilon_0^2 (\epsilon_r^i)^2 c^2 \{A_{2j_1}(k_2 c) + B_{2y_1}(k_2 c)\}^2 \tag{64a}$$

Thus, the total metallic losses for the $TM_{10\ell}$ modes is given by,

$$P'_{m,1} = \frac{8}{3} \sqrt{\frac{\omega\mu_0}{2\sigma}} \omega^2 \epsilon_0^2 [(\epsilon_1^r)^2 a^2 (A_{1j_1}(k_1a) + B_1 y_1(k_1a)) + (\epsilon_2^r)^2 c^2 (A_{1j_1}(k_2c) + B_1 y_1(k_2c))] \quad (64b)$$

Similarly, the metallic losses on metal surfaces for the $TM_{20\ell}$ and $TM_{30\ell}$ modes are given by,

$$P'_{m,2} = \frac{24}{5} \sqrt{\frac{\omega\mu_0}{2\sigma}} \omega^2 \epsilon_0^2 [(\epsilon_1^r)^2 a^2 (A_{1j_2}(k_1a) + B_1 y_2(k_1a)) + (\epsilon_2^r)^2 c^2 (A_{1j_2}(k_2c) + B_1 y_2(k_2c))] \quad (65)$$

$$P'_{m,3} = \frac{48}{7} \sqrt{\frac{\omega\mu_0}{2\sigma}} \omega^2 \epsilon_0^2 [(\epsilon_1^r)^2 a^2 [A_{1j_3}(k_1a) + B_1 y_3(k_1a)] + (\epsilon_2^r)^2 c^2 (A_{1j_3}(k_2c) + B_1 y_3(k_2c))] \quad (66)$$

2.3.4. Dielectric losses for the TM modes

Dielectric losses for the $TM_{10\ell}$, $TM_{20\ell}$ and $TM_{30\ell}$ modes are given by,

$$P'_{d,1} = \omega(W_{1,1}^{TM} + W_{2,1}^{TM}) \tan \delta \quad (67)$$

$$P'_{d,2} = \omega(W_{1,2}^{TM} + W_{2,2}^{TM}) \tan \delta \quad (68)$$

$$P'_{d,3} = \omega(W_{1,3}^{TM} + W_{2,3}^{TM}) \tan \delta \quad (69)$$

2.4. Quality factor

The Quality factor Q is given by

$$Q = \omega \frac{W}{P_m + P_d} \quad (70)$$

where the terms appearing in Eq. (70) have already been explained [1-8,36-41].

2.4.1. Expression of Q for TE modes

For the $TE_{10\ell}$ mode the expression for the Q factor is given by,

$$Q = \omega \frac{W_{1,1}^{TE} + W_{2,1}^{TE}}{P_{m,1} + P_{d,1}} \quad (71)$$

where,

$$W_{1,1}^{TE} = \frac{4}{3} \omega^2 \mu_0^2 \epsilon_0 \epsilon_1^r [A_1^2 r^3 \{j_1^2(k_1r) - j_0(k_1r)j_2(k_1r)\} + B_1^2 r^3 \{y_1^2(k_1r) - y_0(k_1r)y_2(k_1r)\} + A_1 B_1 r^3 \{2y_1(k_1r)j_1(k_1r) - y_0(k_1r)j_2(k_1r) - y_2(k_1r)j_0(k_1r)\}]_a^b$$

$$W_{2,1}^{TE} = \frac{4}{3} \omega^2 \mu_0^2 \epsilon_0 \epsilon_2^r [A_2^2 r^3 \{j_1^2(k_2r) - j_0(k_2r)j_2(k_2r)\} + B_2^2 r^3 \{y_1^2(k_2r) - y_0(k_2r)y_2(k_2r)\} + A_2 B_2 r^3 \{2y_1(k_2r)j_1(k_2r) - y_0(k_2r)j_2(k_2r) - y_2(k_2r)j_0(k_2r)\}]_b^c$$

$$P_{m,1} = \frac{8}{3} \sqrt{\frac{\omega\mu_0}{2\sigma}} \{k_1^2 a^2 \{A_1 j_1'(k_1a) + B_1 y_1'(k_1a)\}^2 + k_2^2 c^2 \{A_2 j_1'(k_2c) + B_2 y_1'(k_2c)\}^2\}$$

$$P_{d,1} = \omega(W_{1,1}^{TE} + W_{2,1}^{TE}) \tan \delta$$

For the $TE_{20\ell}$ mode the expression for the Q factor is given by,

$$Q = \omega \left(\frac{W_{1,2}^{TE} + W_{2,2}^{TE}}{P_{m,2} + P_{d,2}} \right) \quad (72)$$

where,

$$W_{1,2}^{TE} = \frac{12}{5} \omega^2 \mu_0^2 \epsilon_0 \epsilon_1^r [A_1^2 r^3 \{j_2^2(k_1r) - j_1(k_1r)j_3(k_1r)\} + B_1^2 r^3 \{y_2^2(k_1r) - y_1(k_1r)y_3(k_1r)\} + A_1 B_1 r^3 \{2y_2(k_1r)j_2(k_1r) - y_1(k_1r)j_3(k_1r) - y_3(k_1r)j_1(k_1r)\}]_a^b$$

$$W_{2,2}^{TE} = \frac{12}{5} \omega^2 \mu_0^2 \epsilon_0 \epsilon_2^r [A_2^2 r^3 \{j_2^2(k_2r) - j_1(k_2r)j_3(k_2r)\} + B_2^2 r^3 \{y_2^2(k_2r) - y_1(k_2r)y_3(k_2r)\} + A_2 B_2 r^3 \{2y_2(k_2r)j_2(k_2r) - y_1(k_2r)j_3(k_2r) - y_3(k_2r)j_1(k_2r)\}]_b^c$$

$$P_{m,2} = \frac{24}{5} \sqrt{\frac{\omega\mu_0}{2\sigma}} [k_1^2 a^2 \{A_1 j_2'(k_1a) + B_1 y_2'(k_1a)\}^2 + k_2^2 c^2 \{A_2 j_2'(k_2c) + B_2 y_2'(k_2c)\}^2]$$

$$P_{d,2} = \omega(W_{1,2}^{TE} + W_{2,2}^{TE}) \tan \delta$$

Similarly, for the $TE_{30\ell}$ mode the expression for the Q factor becomes,

$$Q = \omega \left(\frac{W_{1,3}^{TE} + W_{2,3}^{TE}}{P_{m,3} + P_{d,3}} \right) \quad (73)$$

where,

$$\begin{aligned} W_{1,3}^{TE} &= \frac{24}{7} \omega^2 \mu_0^2 \epsilon_0 \epsilon_1^r [A_1^2 r^3 \{j_3^2(k_1 r) - j_2(k_1 r) j_4(k_1 r)\} + B_1^2 r^3 \{y_3^2(k_1 r) - y_2(k_1 r) y_4(k_1 r)\} + A_1 B_1 r^3 \{2y_3(k_1 r) j_3(k_1 r) \\ &\quad - y_2(k_1 r) j_4(k_1 r) - y_4(k_1 r) j_2(k_1 r)\}]_a^b \\ W_{2,3}^{TE} &= \frac{24}{7} \omega^2 \mu_0^2 \epsilon_0 \epsilon_2^r [C^2 r^3 \{j_3^2(k_2 r) - j_2(k_2 r) j_4(k_2 r)\} + B^2 r^3 \{y_3^2(k_2 r) - y_2(k_2 r) y_4(k_2 r)\} + A B r^3 \{2y_3(k_2 r) j_3(k_2 r) \\ &\quad - y_2(k_2 r) j_4(k_2 r) - y_4(k_2 r) j_2(k_2 r)\}]_c^d \\ P_{m,3} &= \frac{24}{3} \sqrt{\frac{\omega \mu_0}{2\sigma}} [k_1^2 a^2 \{A_1 j_3'(k_1 a) + B_1 y_3'(k_1 a)\}^2 + k_2^2 c^2 \{A_2 j_3'(k_2 c) + B_2 y_3'(k_2 c)\}^2] \\ P_{d,3} &= \omega (W_{1,3}^{TE} + W_{2,3}^{TE}) \tan \delta \end{aligned}$$

2.4.2. Expressions of Q for the TM modes

Similar to the case for the $TE_{n0\ell}$ modes, the expressions for Q have been derived for the $TM_{n0\ell}$ modes and these are given below:

For the $TM_{10\ell}$ mode,

$$Q = \omega \left(\frac{W_{1,1}^{TM} + W_{2,1}^{TM}}{P'_{m,1} + P'_{d,1}} \right) \quad (74)$$

where,

$$\begin{aligned} W_{1,1}^{TM} &= \frac{4}{3} \omega^2 \mu_0 \epsilon_0^2 (\epsilon_1^r)^2 [A_1^2 r^3 \{j_1^2(k_1 r) - j_0(k_1 r) j_2(k_1 r)\} + B_1^2 r^3 \{y_1^2(k_1 r) - y_0(k_1 r) j_2(k_1 r)\} + A_1 B_1 r^3 \{2j_1(k_1 r) y_1(k_1 r) \\ &\quad - y_0(k_1 r) j_2(k_1 r) - j_0(k_1 r) y_2(k_1 r)\}]_a^b \\ W_{2,1}^{TM} &= \frac{4}{3} \omega^2 \mu_0 \epsilon_0^2 (\epsilon_2^r)^2 [A_2^2 r^3 \{j_1^2(k_2 r) - j_0(k_2 r) j_2(k_2 r)\} + A_2^2 r^3 \{y_1^2(k_2 r) - y_0(k_2 r) y_1(k_2 r)\} + A_2 B_2 r^3 \{2j_1(k_2 r) y_1(k_2 r) \\ &\quad - y_0(k_2 r) j_2(k_2 r) - y_2(k_2 r) j_0(k_2 r)\}]_c^d \\ P'_{m,1} &= \frac{8}{3} \sqrt{\frac{\omega \mu_0}{2\sigma}} \omega^2 \epsilon_0^2 [(\epsilon_1^r)^2 a^2 \{A_1 j_1(k_1 a) + B_1 y_1(k_1 a)\} + (\epsilon_2^r)^2 c^2 \{A_2 j_1(k_2 c) + B_2 y_1(k_2 c)\}] \\ P'_{d,1} &= \omega (W_{1,1}^{TM} + W_{2,1}^{TM}) \tan \delta \end{aligned}$$

For the $TM_{20\ell}$ mode,

$$Q = \omega \left(\frac{W_{1,2}^{TM} + W_{2,2}^{TM}}{P'_{m,2} + P'_{d,2}} \right) \quad (75)$$

$$\begin{aligned} W_{1,2}^{TM} &= \frac{12}{5} \omega^2 \mu_0 \epsilon_0^2 (\epsilon_2^r)^2 [A_1^2 r^3 \{j_2^2(k_1 r) - j_1(k_1 r) j_3(k_1 r)\} + B_1 r^3 \{y_2^2(k_1 r) - y_1(k_1 r) y_3(k_1 r)\} + A_1 B_1 r^3 \{2j_2(k_1 r) y_2(k_1 r) \\ &\quad - y_1(k_1 r) j_3(k_1 r) - j_1(k_1 r) y_3(k_1 r)\}]_a^b \\ W_{2,2}^{TM} &= \frac{12}{5} \omega^2 \mu_0 \epsilon_0^2 (\epsilon_2^r)^2 [A_2^2 r^3 \{j_2^2(k_2 r) - j_1(k_2 r) j_3(k_2 r)\} + B_2 r^3 \{y_2^2(k_2 r) - y_1(k_2 r) y_3(k_2 r)\} + A_2 B_2 r^3 \{2j_2(k_2 r) y_2(k_2 r) \\ &\quad - y_1(k_2 r) j_3(k_2 r) - j_1(k_2 r) y_3(k_2 r)\}]_c^d \\ P'_{m,2} &= \frac{24}{5} \sqrt{\frac{\omega \mu_0}{2\sigma}} \omega^2 \epsilon_0^2 [(\epsilon_1^r)^2 a^2 \{A_1 j_2(k_1 a) + B_1 y_1(k_1 a)\} + (\epsilon_2^r)^2 b^2 \{A_2 j_2(k_2 c) + B_2 y_2(k_2 c)\}] \\ P'_{d,2} &= \omega (W_{1,2}^{TM} + W_{2,2}^{TM}) \tan \delta \end{aligned}$$

and for the $TM_{30\ell}$ mode,

$$Q = \omega \left(\frac{W_{1,3}^{TM} + W_{2,3}^{TM}}{P'_{m,3} + P'_{d,3}} \right) \quad (76)$$

where,

$$\begin{aligned} W_{1,3}^{TM} &= \frac{24}{7} \omega^2 \mu_0 \epsilon_0^2 (\epsilon_1^r)^2 [A_1^2 r^3 \{j_3^2(k_1 r) - j_2(k_1 r) j_4(k_1 r)\} + B_1^2 r^3 \{y_3^2(k_1 r) - y_2(k_1 r) y_4(k_1 r)\} + A_1 B_1 r^3 \{2y_3(k_1 r) j_3(k_1 r) \\ &\quad - y_2(k_1 r) j_4(k_1 r) - j_2(k_1 r) y_4(k_1 r)\}]_a^b \\ W_{2,3}^{TM} &= \frac{24}{7} \omega^2 \mu_0 \epsilon_0^2 (\epsilon_2^r)^2 [A_2^2 r^3 \{j_3^2(k_2 r) - j_2(k_2 r) j_4(k_2 r)\} + B_2^2 r^3 \{y_3^2(k_2 r) - y_2(k_2 r) y_4(k_2 r)\} + A_1 B_1 r^3 \{2y_3(k_2 r) j_3(k_2 r) \\ &\quad - y_2(k_2 r) j_4(k_2 r) - j_2(k_2 r) y_4(k_2 r)\}]_c^d \\ P'_{m,3} &= \frac{48}{7} \omega^2 \epsilon_0^2 \sqrt{\frac{\omega \mu_0}{2\sigma}} \{(\epsilon_1^r)^2 a^2 (A_1 j_3(k_1 a) + B_1 y_3(k_1 a))^2 + \epsilon_2^r c^2 (A_2 j_3(k_2 c) + B_2 y_3(k_2 c))^2\} \\ P'_{d,3} &= \omega (W_{1,3}^{TM} + W_{2,3}^{TM}) \tan \delta \end{aligned}$$

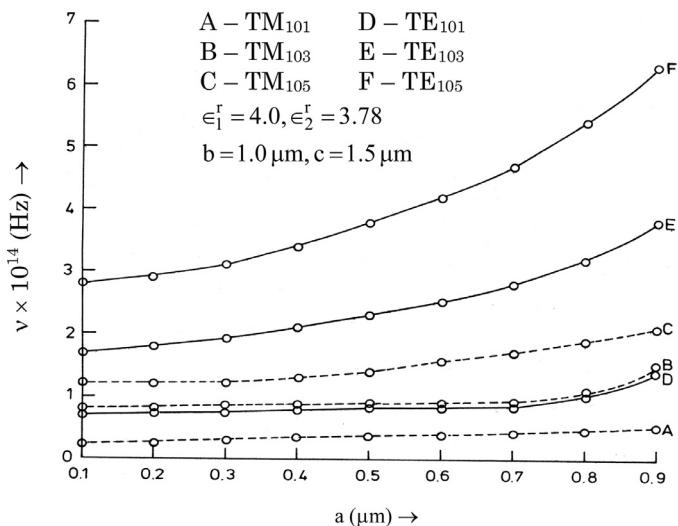


Fig. 2. Variation of Resonant frequency with radius for TM_{101} , TM_{103} , TM_{105} , TE_{101} , TE_{103} and TE_{105} modes.

3. Results and discussions

3.1. Resonant frequencies

The spherical Bessel functions $j_n(x)$ and $y_n(x)$ have been used to solve characteristic Eqs. (9) and (15) for the TE and TM modes. A mode with a given value of n is $n+1$ fold degenerate i.e. $(n+1)$ modes have the same resonant frequency. In this case also five roots ($\ell = 1-5$) for each of Eqs. (9) and (15) have been determined and the resonant frequencies have been calculated for the $TE_{nm\ell}$ and $TM_{nm\ell}$ modes ($n = 1-3$; $\ell = 1-5$) using $\epsilon_1^r = 4.0$ and $\epsilon_2^r = 3.78$, $a = 0.1-0.9 \mu\text{m}$, $b = 1.0-9.5 \mu\text{m}$ and $c = 1.5-10.0 \mu\text{m}$. In this case the value of a is limited by the value of b (radius of the inner dielectric sphere). Resonant frequency has been computed as a function of one of the three radii a , b and c keeping the other two constant.

Fig. 2 shows variation of the resonant frequency with a for the $TE_{nm\ell}$ and $TM_{nm\ell}$ modes.

It is observed that when the concentric metallic sphere radius a is increased from $0.1 \mu\text{m}$ to $0.9 \mu\text{m}$ with $b = 1.0 \mu\text{m}$ and $c = 1.5 \mu\text{m}$, the resonant frequency increases monotonically. However, increase is slow due to the fact that the inner radius cannot exceed $1 \mu\text{m}$ (the value of b) and the outer radius c is $1.5 \mu\text{m}$. Hence a is of resonator studied in shielded dielectric spherical shell resonator [36–40]. By changing the radius b of the inner dielectric sphere no appreciable change in frequency is observed due to small difference in the permittivities of the materials of the inner and the outer dielectric spheres.

Fig. 3 shows variation of the resonant frequency with c for the $TE_{10\ell}$ and $TM_{10\ell}$ modes.

It can be seen that when we increase the radius c of the outer dielectric sphere, the resonant frequency of the shielded composite dielectric resonator decreases monotonically.

3.2. Quality factors

With the help of Eqs. (74) and (76) we have calculated the quality factors for the $TE_{10\ell}$ and $TM_{10\ell}$ modes.

Fig. 4 shows the variation of the quality factor with the radius c of the outer dielectric sphere for the $TE_{10\ell}$ and $TM_{10\ell}$ modes.

When the outer radius (c) of the shielded composite dielectric spherical shell resonator increases the quality factor Q of the resonator increases monotonically. Effect of the radius (a) of the inner

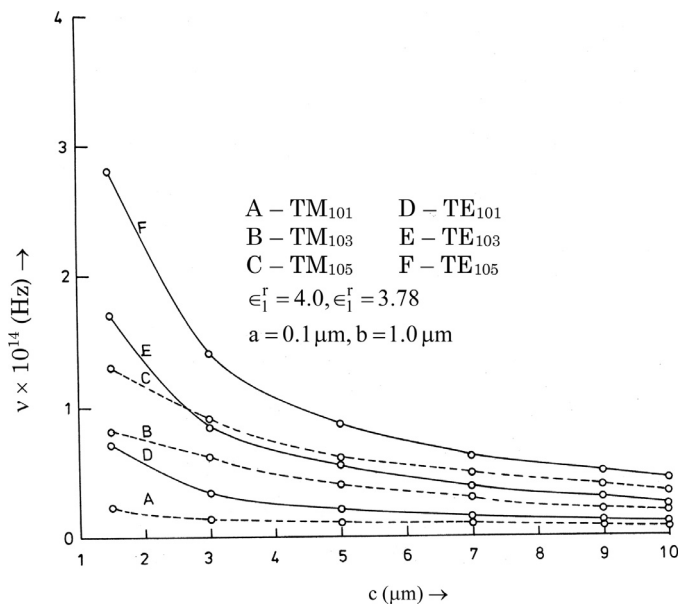


Fig. 3. Variation of resonant frequency with radius for TM_{101} , TM_{103} , TM_{105} , TE_{101} , TE_{103} and TE_{105} Mode.

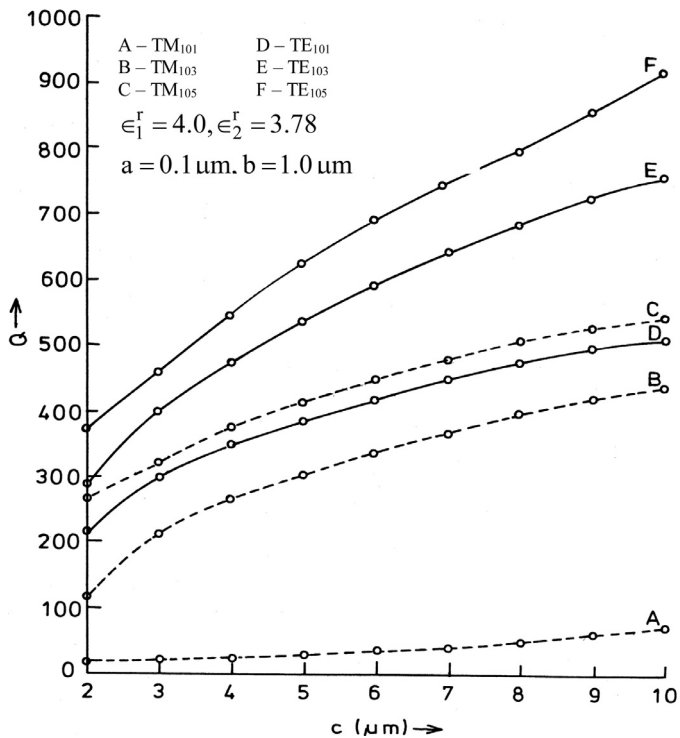


Fig. 4. Variation of Q -factor with radius for TM_{101} , TM_{103} , TM_{105} , TE_{101} , TE_{103} and TE_{105} modes.

metal sphere on the quality factor has also been studied. Similar to the case of the resonator studied in shielded dielectric spherical shell resonator [22,23], here also a could be varied in a very limited range due to its strong effect on the Q values. By increasing the size of the inner concentric metal sphere the quality factor is reduced significantly. It is found that when the radius a of the inner metal sphere is increased from $0.1 \mu\text{m}$ to $0.5 \mu\text{m}$ with $b = 1.0 \mu\text{m}$, $c = 1.5 \mu\text{m}$ the quality factor drops from 138 to 28 for the TE_{101} mode. It is to be noted here that the quality factor decreases with increasing radius a for $TE_{n0\ell}$ and $TM_{n0\ell}$ modes. It

is observed that when the radius a is increased from 0.1 mm to 0.9 mm with fixed values of b (=1.0 mm) and c (=1.5 mm), the quality factor varies in the range 59–1228 for $TE_{n\ell}$ modes and in the range 66–1166 for $TM_{n\ell}$ modes ($n=1-3$, $\ell=1-5$).

3. Conclusions

In the present paper, an electromagnetic field analysis of the composite dielectric spherical shell resonators has been studied in details. It is found that when the outer radius (c) of the shielded composite dielectric spherical shell resonator increases the quality factor Q of the resonator increases monotonically. This high value of quality factor (Q) of the dielectric resonators have been used as stabilizing devices for oscillators in microwave integrated circuits. It is also the resonant frequencies, field distributions and Q -factors for particular modes ($TE_{n\ell}$ and $TM_{n\ell}$) in dielectric resonators on micro-strip substrates or supporters, and with or without tuning devices, have to be efficiently obtained. Thus, the studies of shielded multilayer dielectric composite resonators indicate the possibilities of increasing their Q -factors and improving their spectral characteristics. It is also observed that by an introducing of an inner concentric superconducting sphere within a dielectric spherical resonator is a more effective controlling parameter for the resonant frequency than the other parameters.

Acknowledgements

Authors are thankful to the staff members, Computer Center, Banaras Hindu University for their help during the computational work.

Appendices

Appendix - A

Spherical polar coordinates (r , θ and ϕ)

The spherical polar-coordinates system consists of the following:

- (i) Concentric spheres centered at the origin,

$$r = \sqrt{x^2 + y^2 + z^2} = \text{constant.} \quad (\text{A1})$$

- (ii) Right circular cones centered on the z -(polar) axis, vertices at the origin,

$$\theta = \arccos \frac{z}{\sqrt{x^2 + y^2 + z^2}} = \text{constant.} \quad (\text{A2})$$

- (iii) Half planes through the z -(polar) axis,

$$\phi = \arctan \frac{y}{x} = \text{constant.} \quad (\text{A3})$$

In spherical polar coordinate system there lies symmetry about a point. The position of any point P is specified in spherical coordinate r , θ and ϕ , as shown in Fig. A.1(a). \hat{r} , $\hat{\theta}$ and $\hat{\phi}$ are the unit vector which of perpendicular to each other and from a right handed triad of unit vectors. Fig. A.1(b) shows that

$$\text{the line element} \quad dr = \hat{r} dr + \hat{\theta} r d\theta + \hat{\phi} r \sin \theta d\phi, \quad (\text{A4})$$

$$\text{the area element} \quad dA = r^2 \sin \theta d\theta d\phi \quad (\text{A5})$$

$$\text{and the volume element} \quad dV = r^2 \sin \theta dr d\theta d\phi \quad (\text{A6})$$

The Cartesian and spherical polar coordinate are related as,

$$\begin{aligned} x &= r \sin \theta \cos \phi \\ y &= r \sin \theta \sin \phi \\ z &= r \cos \theta \end{aligned} \quad (\text{A7})$$

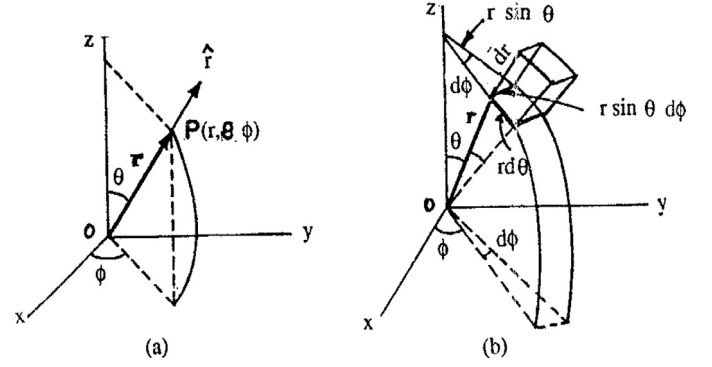


Fig. A.1. Spherical polar coordinates.

∇ Operations in spherical polar coordinates

The basic ∇ operations in spherical polar coordinates are given below,

$$\nabla \psi = \hat{r} \frac{\partial \psi}{\partial r} + \hat{\theta} \frac{1}{r} \frac{\partial \psi}{\partial \theta} + \hat{\phi} \frac{1}{r \sin \theta} \frac{\partial \psi}{\partial \phi} \quad (\text{A8})$$

$$\nabla \cdot \vec{A} = \frac{1}{r^2} \frac{\partial}{\partial r} (r^2 A_r) + \frac{1}{r \sin \theta} \frac{\partial}{\partial \theta} (\sin \theta A_\theta) + \frac{1}{r \sin \theta} \frac{\partial A_\phi}{\partial \phi} \quad (\text{A9})$$

$$\nabla^2 \psi = \frac{1}{r^2} \frac{\partial}{\partial r} \left(r^2 \frac{\partial \psi}{\partial r} \right) + \frac{1}{r^2 \sin \theta} \frac{\partial}{\partial \theta} \left(\sin \theta \frac{\partial \psi}{\partial \theta} \right) + \frac{1}{r^2 \sin^2 \theta} \frac{\partial^2 \psi}{\partial \phi^2} \quad (\text{A10})$$

$$\nabla \times \vec{A} = \frac{1}{r^2 \sin \theta} \begin{vmatrix} \hat{r} & r \hat{\theta} & r \sin \theta \hat{\phi} \\ \frac{\partial}{\partial r} & \frac{\partial}{\partial \theta} & \frac{\partial}{\partial \phi} \\ A_r & r A_\theta & \sin \theta A_\phi \end{vmatrix} \quad (\text{A11})$$

Vector identities

Several important vector identities are given below:

$$\nabla \cdot (\psi \vec{A}) = \vec{A} \cdot \nabla \psi + \psi \nabla \cdot \vec{A} \quad (\text{A12})$$

$$\nabla \times (\psi \vec{A}) = \nabla \psi \times \vec{A} + \psi \nabla \times \vec{A} \quad (\text{A13})$$

$$\nabla \times (\nabla \times \vec{A}) = \nabla (\vec{A} \cdot \nabla) + \nabla^2 \vec{A} \quad (\text{A14})$$

$$\nabla \cdot \nabla \psi = \nabla^2 \psi \quad (\text{A15})$$

Appendix - B

Legendre's polynomial

Legendre differential equation of order n is

$$(1 - x^2) \frac{d^2 \psi}{dx^2} - 2x \frac{d\psi}{dx} + n(n+1) \psi = 0 \quad (\text{B1})$$

where n is a positive integer or zero. The equation of such type can be solved in series of ascending or descending power of x . The solution of the Legendre's differential equation are given by,

- (i) For even n ,

$$P_n(x) = A_n \left[1 - n(n+1) \frac{x^2}{2!} - n(n+1) \{2.3 - n(n+1)\} \frac{x^4}{4!} - n(n+1) \{2.3 - n(n+1)\} \{4.5 - n(n+1)\} \frac{x^6}{6!} \dots \dots \right] \quad (\text{B2})$$

(ii) For odd n ,

$$P_n(x) = A_n \left[x + \{1.2 - n(n+1)\} \frac{x^3}{3!} + \{1.2 - n(n+1)\} \{3.4 - n(n+1)\} \frac{x^5}{5!} + \dots \right] \tag{B3}$$

Legendre's Polynomials $P_n(x)$ for some order are given below,

$$\left. \begin{aligned} P_0(x) &= 1 \\ P_1(x) &= x \\ P_2(x) &= \frac{1}{2}(3x^2 - 1) \\ P_3(x) &= \frac{1}{2}(5x^3 - 3x) \\ P_4(x) &= \frac{1}{8}(35x^4 - 30x^2 + 3x) \end{aligned} \right\} \tag{B4}$$

Associated Legendre's polynomial

The differential equation

$$(1 - x^2) \frac{d^2\psi}{dx^2} - 2x \frac{d\psi}{dx} + \left\{ n(n+1) - \frac{m^2}{1-x^2} \right\} \psi = 0 \tag{B5}$$

is called Legendre's associated equation of order n . Substituting $x = \cos\theta$, Eq. (B5) takes the form,

$$\frac{d^2\psi}{d\theta^2} + \cot\theta \frac{d\psi}{d\theta} + \left\{ n(n+1) - \frac{m^2}{\sin^2\theta} \right\} \psi(\theta) = 0 \tag{B6}$$

The solution of above Eq. (B5) is given by,

$$P_n^m(x) = (1-x^2)^{m/2} \frac{d^m}{dx^m} P_n(x) \tag{B7}$$

$P_n^m(x)$ is called associated Legendre polynomial of the first kind. The associated Legendre polynomials of the second kind $Q_n^m(x)$ is also solution of Eq. (B5) and it is given by,

$$Q_n^m(x) = (-1)^n (1-x^2)^{m/2} \frac{d^m}{dx^m} Q_n(x) \tag{B8}$$

However, $Q_n^m(x)$ solution of Eq. (B5) is not of our interest. From the definition of associated Legendre polynomial, given by Eq. (B7), it is clear that

$$P_n^0(x) = P_n(x) \tag{B9}$$

$$\left. \begin{aligned} P_1^0(x) &= P_1(x) = x = \cos\theta \\ P_2^0(x) &= P_2(x) = \frac{1}{2}(3x^2 - 1) = \frac{1}{2}(3\cos^2\theta - 1) \\ P_3^0(x) &= P_3(x) = \frac{1}{2}(5x^3 - 3x) = \frac{1}{2}(5\cos^3\theta - 3\cos\theta) \end{aligned} \right\} \tag{B10}$$

Expressions for some associated Legendre's polynomial are given are given below,

$$\left. \begin{aligned} P_0^0(\cos\theta) &= 1, & P_2^2(\cos\theta) &= 3\sin^2\theta \\ P_1^0(\cos\theta) &= \cos\theta, & P_3^0(\cos\theta) &= \frac{1}{2}\cos\theta(5\cos^2\theta - 3) \\ P_1^1(\cos\theta) &= \sin\theta, & P_3^1(\cos\theta) &= \frac{3}{2}\sin\theta(5\cos^2\theta - 1) \\ P_2^0(\cos\theta) &= \frac{1}{2}(3\cos^2\theta - 1), & P_3^2(\cos\theta) &= 15\cos\theta\sin^2\theta \\ P_2^1(\cos\theta) &= 3\cos\theta\sin\theta, & P_3^3(\cos\theta) &= 15\sin^3\theta \end{aligned} \right\} \tag{B11}$$

$$P_n^{m+1}(x) - \frac{2mx}{(1-x^2)^{\frac{1}{2}}} P_n^m(x) + [n(n+1) - m(m-1)] P_n^{m-1}(x) = 0 \tag{B12}$$

$$(1-x^2)^{\frac{1}{2}} P_n^{m'}(x) = \frac{1}{2} P_n^{m+1}(x) - \frac{1}{2} (n+m)(n-m+1) P_n^{m-1}(x)$$

(B13)

The dash on P in Eq. (B13) denotes its derivative with respect to argument x .

Appendix - C

Bessel's functions

The differential equation

$$\frac{d^2\psi}{dz^2} + \frac{1}{z} \frac{d\psi}{dz} + \left(1 - \frac{p^2}{z^2}\right) \psi = 0 \tag{C1}$$

is called Bessel's differential equation of order p .

This equation has a non-essential singularity at the point $z=0$ and therefore its solution can be obtained as a power Series developed about this point. Series solution of Eq. (C1) is given by,

$$J_p(z) = \frac{z^p}{2^p p!} \left\{ 1 - \frac{z^2}{2^2 1!(p+1)} + \frac{z^4}{2^4 2!(p+1)(p+2)} \dots \dots \dots + \frac{(-1)^r z^{2r}}{2^{2r} r!(p+1)(p+2)\dots(p+r)} + \dots \dots \dots \right\} \tag{C2}$$

where $J_p(z)$ is called the Bessel function of the first kind of order p .

The Second solution of Bessel's Eq. (C1) is given by,

$$Y_p(z) = \frac{2}{\pi} \{ \gamma + \log(Z/2) \} J_p(z) - \frac{1}{\pi} \sum_{q=0}^{p-1} \frac{(p-q-1)!}{q!} \left(\frac{Z}{2}\right)^{2q-p} - \frac{1}{\pi} \sum_{q=0}^{\infty} \frac{(-1)^q}{q!(p-q)!} \left(\frac{Z}{2}\right)^{p+2q} \left(1 + \frac{1}{2} + \frac{1}{3} + \dots + \frac{1}{q} + \dots + 1 + \frac{1}{2} + \dots + \frac{1}{p+q}\right) \tag{C3}$$

where γ is usual Euler's Mascheroni constant. $Y_p(z)$ is called the Bessel function of the second kind of order p . Therefore, the complete general solution of Bessel's differential equation is

$$y = AJ_p(z) + BY_p(z) \tag{C4}$$

where A and B are any constants.

Recurrence relations for Bessel's functions

$$2p J_p(z) = z \{ J_{p-1}(z) + J_{p+1}(z) \} \tag{C5}$$

$$2J'_p(z) = J_{p-1}(z) - J_{p+1}(z) \tag{C6}$$

$$zJ'_p(z) = J_{p-1}(z) - pJ_p(z) \tag{C7}$$

$$zJ'_p(z) = pJ_p(z) - zJ_{p+1}(z) \tag{C8}$$

where dash denotes differentiation with respect to the argument.

Spherical Bessel functions

The spherical Bessel functions are defined as solution of differential equation

$$r^2 \frac{d^2R}{dr^2} + 2r \frac{dR}{dr} + [k^2 r^2 - n(n+1)] R = 0 \tag{C9}$$

Which is the radial equation obtained by separating the spherical polar coordinate of Helmholtz equation. Constant k occurs in Helmholtz equation and integer n is a separation constant. This equation is not Bessel equation but can be reduced to Bessel equation by the substitution

$$R(kr) = \frac{Z_{n+\frac{1}{2}}(kr)}{\sqrt{kr}} \tag{C10}$$

Then Eq. (C9) becomes

$$r^2 \frac{d^2 Z}{dr^2} + r \frac{dZ}{dr} + \left[k^2 r^2 - \left(n + \frac{1}{2} \right)^2 \right] Z = 0 \tag{C11}$$

Which is Bessel's equation, where z is a Bessel function of order $(n + \frac{1}{2})$ for integer n .

Relations between Bessel's functions and spherical Bessel's functions

The relations between Bessel's function and Spherical Bessel's functions of the first kind $j_n(x)$ and second kind $y_n(x)$ are given as below,

$$J_{n+\frac{1}{2}}(x) = \sqrt{2x/\pi} j_n(x) \tag{C12}$$

$$Y_{n+\frac{1}{2}}(x) = \sqrt{2x/\pi} y_n(x) \tag{C13}$$

Some useful relation involving Bessel's function and spherical Bessel's functions

$$J_{n+\frac{1}{2}}(x) + 2xJ'_{n+\frac{1}{2}}(x) = \sqrt{\frac{8x}{\pi}} \{j_n(x) + xj'_n(x)\} \tag{C14}$$

$$Y_{n+\frac{1}{2}}(x) + 2xY'_{n+\frac{1}{2}}(x) = \sqrt{\frac{8x}{\pi}} \{y_n(x) + xy'_n(x)\} \tag{C15}$$

$$\int_0^a J_p^2(kr) \cdot r dr = \frac{a^2}{2} \left\{ J_p^2(ka) + \left(1 - \frac{p^2}{k^2 a^2} \right) J_p^2(ka) \right\} \tag{C16}$$

$$\int_b^a J_p(kr) Y_p(kr) r dr = \left[\frac{r^2}{2} \left\{ J'_p(kr) Y_p(kr) + \left(1 - \frac{p^2}{k^2 r^2} \right) J_p(kr) Y_p(kr) \right\} \right]_b^a \tag{C17}$$

$$j_{n+1}(x) = -x^n \frac{d}{dx} \left\{ \frac{j_n(x)}{x} \right\} \tag{C18}$$

$$y_{n+1}(x) = -y^n \frac{d}{dx} \left\{ \frac{y_n(x)}{x} \right\} \tag{C19}$$

$$j'_n(x) = j_{n-1}(x) - \frac{(n+1)}{x} j_n(x) \tag{C20}$$

$$y'_n(x) = y_{n-1}(x) - \frac{(n+1)}{x} y_n(x) \tag{C21}$$

$$j_n(x) + xj'_n(x) = xj_{n-1}(x) - nj_n(x) \tag{C22}$$

$$y_n(x) + xy'_n(x) = xy_{n-1}(x) - ny_n(x) \tag{C23}$$

The dash on J and j denotes derivative with respect to the argument (Tables 1-3).

Table 1
Expression for $j_n(x)$.

n	$j_n(x)$
0	$\frac{\sin x}{x}$
1	$\frac{\sin x}{x^2} - \frac{\cos x}{x}$
2	$\frac{\sin x}{x^3} \left(\frac{3}{x^2} - 1 \right) - \frac{3 \cos x}{x^2}$
3	$\frac{\sin x}{x^4} \left(\frac{15}{x^3} - \frac{6}{x} \right) + \frac{\cos x}{x} \left(1 - \frac{15}{x^2} \right)$
4	$\frac{\sin x}{x^5} \left(1 - \frac{45}{x^2} + \frac{105}{x^4} \right) + \frac{\cos x}{x} \left(\frac{10}{x} - \frac{105}{x^3} \right)$
5	$\frac{\sin x}{x^6} \left(\frac{15}{x} - \frac{420}{x^3} + \frac{945}{x^5} \right) + \frac{\cos x}{x} \left(-1 + \frac{105}{x^2} - \frac{945}{x^4} \right)$
6	$\frac{\sin x}{x^7} \left(-1 + \frac{210}{x^2} - \frac{4725}{x^4} + \frac{10395}{x^6} \right) + \frac{\cos x}{x} \left(-\frac{21}{x} + \frac{1260}{x^3} - \frac{10395}{x^5} \right)$

Table 2
Expression for $y_n(x)$.

n	$y_n(x)$
0	$-\frac{\cos x}{x}$
1	$-\frac{\sin x}{x} - \frac{\cos x}{x^2}$
2	$-\frac{3 \sin x}{x^2} + \frac{\cos x}{x} \left(1 - \frac{3}{x^2} \right)$
3	$\frac{\sin x}{x} \left(1 - \frac{15}{x^2} \right) + \frac{\cos x}{x} \left(\frac{6}{x} - \frac{15}{x^3} \right)$
4	$\frac{\sin x}{x} \left(\frac{10}{x} - \frac{105}{x^3} \right) + \frac{\cos x}{x} \left(-1 + \frac{45}{x^2} - \frac{105}{x^4} \right)$
5	$\frac{\sin x}{x} \left(-1 + \frac{105}{x^2} - \frac{945}{x^4} \right) + \frac{\cos x}{x} \left(-\frac{15}{x} + \frac{420}{x^3} - \frac{945}{x^5} \right)$
6	$\frac{\sin x}{x} \left(-\frac{21}{x} + \frac{1260}{x^3} - \frac{10395}{x^5} \right) + \frac{\cos x}{x} \left(1 - \frac{210}{x^2} + \frac{4725}{x^4} - \frac{10395}{x^6} \right)$

Table 3
Expression $\frac{d}{dx} \{xj_n(x)\}$.

n	$\frac{d}{dx} \{xj_n(x)\}$
1	$\frac{\sin x}{x} \left(x - \frac{1}{x} \right) + \frac{\cos x}{x}$
2	$\frac{\sin x}{x} \left(3 - \frac{6}{x^2} \right) + \frac{\cos x}{x} \left(-x + \frac{6}{x} \right)$
3	$\frac{\sin x}{x} \left(-x + \frac{21}{x} - \frac{45}{x^3} \right) + \frac{\cos x}{x} \left(6 - \frac{45}{x^2} \right)$
4	$\frac{\sin x}{x} \left(10 - \frac{195}{x^2} + \frac{420}{x^4} \right) - \frac{\cos x}{x} \left(x - \frac{55}{x} + \frac{420}{x^3} \right)$
5	$\frac{\sin x}{x} \left(x - \frac{120}{x} + \frac{2205}{x^3} - \frac{4725}{x^5} \right) + \frac{\cos x}{x} \left(15 - \frac{630}{x^2} + \frac{4725}{x^4} \right)$
6	$\frac{\sin x}{x} \left(21 - \frac{1680}{x^2} + \frac{29295}{x^4} - \frac{62370}{x^6} \right) + \frac{\cos x}{x} \left(-x + \frac{231}{x} - \frac{8505}{x^3} + \frac{62370}{x^5} \right)$

Appendix - D

In the present work eigen modes of a spherical homogeneous and isotropic dielectric resonator enclosed in a metallic spherical shell are determined using straightforward procedure. In a source-free homogeneous isotropic dielectric medium the four Maxwell's equations are given by,

$$\nabla \cdot \vec{D} = 0 \tag{D.1}$$

$$\nabla \cdot \vec{B} = 0 \tag{D.2}$$

$$\nabla \times \vec{E} = -\frac{\partial \vec{B}}{\partial t} \tag{D.3}$$

$$\nabla \times \vec{H} = \frac{\partial \vec{D}}{\partial t} \tag{D.4}$$

The following equations give constitutive relations between the electric field vector \vec{E} and the electric displacement vector \vec{D} and the magnetic field vector \vec{H} and the magnetic induction vector \vec{B} ,

$$\vec{D} = \epsilon \vec{E} = \epsilon_r \epsilon_0 \vec{E} \tag{D.5}$$

$$\vec{B} = \mu \vec{H} = \mu_r \mu_0 \vec{H} \tag{D.6}$$

Here ϵ_0 and μ_0 represent respectively the electric permittivity and magnetic permeability of the free space, ϵ and μ are the corresponding quantities for the dielectric material and $\epsilon_r = \epsilon/\epsilon_0$, $\mu_r = \mu/\mu_0$. For a non-magnetic dielectric material $\mu_r = 1$. Therefore, one has

$$\vec{B} = \mu_0 \vec{H} \tag{D.7}$$

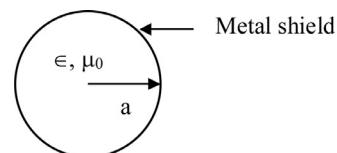


Fig. D.1. Shielded homogeneous isotropic spherical dielectric resonator.

Assuming $e^{j\omega t}$ time dependence for the electric field vector \vec{E} and the magnetic field vector \vec{H} and using Eqs. (D.5) and (D.6), Eqs. (D.1)–(D.4) are simplified to give,

$$\vec{\nabla} \cdot \vec{E} = 0 \quad (D.8)$$

$$\vec{\nabla} \cdot \vec{H} = 0 \quad (D.9)$$

$$\vec{\nabla} \times \vec{E} = -j\omega\mu_0\vec{H} \quad (D.10)$$

$$\vec{\nabla} \times \vec{H} = j\omega\epsilon_0\epsilon_r\vec{E} \quad (D.11)$$

Using expressions for curl in spherical polar coordinates system (Appendix-A, Eq. (A11)) Eqs. (D.10) and (D.11) can be solved to give the expressions for the field components $H_r, H_\theta, H_\phi; E_r, E_\theta,$ and E_ϕ .

$$H_r = -\frac{1}{j\omega\mu_0 r^2 \sin\theta} \left\{ \frac{\partial}{\partial\theta} (r \sin\theta E_\phi) - \frac{\partial}{\partial\phi} (r E_\theta) \right\} \quad (D.12)$$

$$H_\theta = -\frac{1}{j\omega\mu_0 r \sin\theta} \left\{ \frac{\partial}{\partial\phi} (E_r) - \frac{\partial}{\partial r} (r \sin\theta E_\phi) \right\} \quad (D.13)$$

$$H_\phi = -\frac{1}{j\omega\mu_0 r} \left\{ \frac{\partial}{\partial r} (r E_\theta) - \frac{\partial}{\partial\theta} (E_r) \right\} \quad (D.14)$$

$$E_r = \frac{1}{j\omega\epsilon_0\epsilon_r r^2 \sin\theta} \left\{ \frac{\partial}{\partial\theta} (r \sin\theta H_\phi) - \frac{\partial}{\partial\phi} (r H_\theta) \right\} \quad (D.15)$$

$$E_\theta = \frac{1}{j\omega\epsilon_0\epsilon_r r \sin\theta} \left\{ \frac{\partial}{\partial\phi} (H_r) - \frac{\partial}{\partial r} (r \sin\theta H_\phi) \right\} \quad (D.16)$$

$$E_\phi = \frac{1}{j\omega\epsilon_0\epsilon_r r} \left\{ \frac{\partial}{\partial r} (r H_\theta) - \frac{\partial}{\partial\theta} (H_r) \right\} \quad (D.17)$$

Eqs. (D.12)–(D.14) can be used to find magnetic field components provided the electric field components are known. Similarly, Eqs. (D.15)–(D.17) can be used to find electric field components provided the magnetic field components are known. If one takes the curl of Eq. (D.10) one gets,

$$\begin{aligned} \vec{\nabla} \times (\vec{\nabla} \times \vec{E}) &= -j\omega\mu_0 (\vec{\nabla} \times \vec{H}) \\ \vec{\nabla} (\vec{\nabla} \cdot \vec{E}) - \nabla^2 (\vec{E}) &= -j\omega\mu_0 (\vec{\nabla} \times \vec{H}) \end{aligned} \quad (D.18)$$

Using Eqs. (D.8) and (D.11) the following differential equation for the electric field vector \vec{E} is obtained as,

$$(\nabla^2 + \omega^2 \mu_0 \epsilon_0 \epsilon_r) \vec{E} = 0 \quad (D.19)$$

Similarly, taking the curl of Eq. (D.11) and using Eqs. (D.9) and (D.10), the differential equation for the magnetic field vector \vec{H} is obtained as,

$$(\nabla^2 + \omega^2 \mu_0 \epsilon_0 \epsilon_r) \vec{H} = 0 \quad (D.20)$$

Eqs. (D.19) and (D.20) represent differential equations for the electric vector \vec{E} and the magnetic vector \vec{H} respectively. To solve Eqs. (D.19) and (D.20) the procedure followed by [39–40] which appears to be rather clumsy. In the present work we use the standard theory [39–40] to find the electric field and magnetic field vectors for the TE_{nml} and the TM_{nml} modes separately. For the TE_{nml} mode the following condition is satisfied by the electric field vector \vec{E} ,

$$\vec{r} \cdot \vec{E} = 0 \quad (D.21)$$

Validity of Eq. (D.21) suggests that the electric field \vec{E} can be written in terms of the gradient of some scalar function ψ as,

$$\vec{E} = \vec{r} \times \vec{\nabla} \psi \quad (D.22)$$

Replacing \vec{E} in Eq. (D.21) by the expression on the RHS of Eq. (D.22) satisfies Eq. (D.21). Hence, Eq. (D.22) gives the general expression for the electric field vector \vec{E} . Here ψ is any well behaved scalar field that satisfies the Helmholtz equation. The Helmholtz equation for ψ is given by,

$$(\nabla^2 + k^2) \psi = 0 \quad (D.23)$$

where ψ is some scalar function of the co-ordinates r, θ and ϕ i.e. $\psi = \psi(r, \theta, \phi)$. The expression of ∇^2 in the spherical polar coordinate system is given by

$$\nabla^2 \psi = \frac{1}{r^2 \sin\theta} \left\{ \sin\theta \frac{\partial}{\partial r} (r^2 \frac{\partial \psi}{\partial r}) + \frac{\partial}{\partial \theta} (\sin\theta \frac{\partial \psi}{\partial \theta}) + \frac{1}{\sin\theta} \frac{\partial^2 \psi}{\partial \theta^2} \right\} \quad (D.24)$$

Now assuming $\psi(r, \theta, \phi) = R(r) \Theta(\theta) \Phi(\phi)$, and employing the method of separation of variables, Eq. (D.23) gives,

$$\begin{aligned} r^2 \sin^2 \theta \ddot{R} + 2r \sin^2 \theta \dot{R} + \sin^2 \theta \ddot{\Theta} + \sin\theta \cos\theta \dot{\Theta} + \frac{\ddot{\Phi}}{\Phi} \\ + \omega^2 \epsilon_0 \mu_0 \epsilon_r r^2 \sin^2 \theta = 0 \end{aligned} \quad (D.25)$$

where single dot denotes the first derivative with respect to r, θ and ϕ and the double dots denotes the second derivative with respect to r, θ and ϕ . Now as the variable ϕ occurs in $\ddot{\Phi}(\phi)/\Phi(\phi)$ only, it can be replaced by some constant, say, $-m^2$ i.e.

$$\frac{\ddot{\Phi}(\phi)}{\Phi(\phi)} + m^2 = 0 \quad (D.26)$$

The symbol m appearing in Eq. (D.26) can take integral values only due to the reason given after Eq. (D.34). The solutions of Eq. (D.26) are given by

$$\left\{ \Phi(\phi) \sim \begin{matrix} \cos m\phi \\ \sin m\phi \end{matrix} \right\} \quad (D.27)$$

Replacing $\ddot{\Phi}(\phi)/\Phi(\phi)$ by $-m^2$ in Eq. (D.25) it reduces to the following form,

$$\frac{r^2}{R} \left\{ \ddot{R} + \frac{2}{r} \dot{R} + \omega^2 \epsilon_0 \mu_0 \epsilon_r R \right\} + \frac{1}{\Theta} \left\{ \ddot{\Theta} + \cot\theta \dot{\Theta} - \frac{m^2 \Theta}{\sin^2 \theta} \right\} = 0 \quad (D.28)$$

In Eq. (D.28) since the terms in the first pair of brackets is a function of r only and the terms in the second pair of brackets is a function of θ only, the two bracketed terms can separately be equated to constants. Let the first bracketed term be replaced by a constant $n(n+1)$ then Eq. (D.28) splits into the following two equations as,

$$\ddot{\Theta} + \dot{\Theta} \cot\theta + \left\{ n(n+1) - \frac{m^2}{\sin^2 \theta} \right\} \Theta = 0 \quad (D.29)$$

$$\ddot{R} + \frac{2}{r} \dot{R} + \left\{ \omega^2 \mu_0 \epsilon_0 \epsilon_r - \frac{n(n+1)}{r^2} \right\} R = 0 \quad (D.30)$$

The solutions of Eq. (D.29) are associated Legendre Polynomials $P_n^m(\cos\theta)$ and $Q_n^m(\cos\theta)$ (Appendix-B). However, $Q_n^m(\cos\theta)$ has singularities at $\cos\theta = \pm 1$, leading to infinite values of ψ , which will lead to infinite values of the electromagnetic field vectors \vec{E} and \vec{H} . Therefore, the acceptable solution of Eq. (D.29) is given by,

$$\Theta(\theta) \sim P_n^m(\cos\theta) \quad (D.31)$$

In order to find solution of Eq. (D.30) let us substitute $X = R\sqrt{r}$ in Eq. (D.30). By this substitution Eq. (D.30) reduces to,

$$\ddot{X} + \frac{\dot{X}}{r} + \left\{ \omega^2 \mu_0 \epsilon_0 \epsilon_r - \frac{(n+\frac{1}{2})^2}{r^2} \right\} X = 0 \quad (D.32)$$

Here, the dots denote derivatives with respect to r . Eq. (D.32) is Bessel's differential equation of order $(n + \frac{1}{2})$ (Appendix-C). On changing the variable from r to $(\sqrt{\omega^2 \mu_0 \epsilon_0 \epsilon_r})r = (\omega \sqrt{\mu_0 \epsilon_0 \epsilon_r})r = (\frac{\omega}{c} \sqrt{\epsilon_r})r = kr$, where $c = \frac{1}{\sqrt{\mu_0 \epsilon_0}}$ is the speed of light in vacuum, Eq. (D.32) has the solutions of the form $J_{n+\frac{1}{2}}(kr)$ or $Y_{n+\frac{1}{2}}(kr)$ or a linear combination of these two Bessel functions. Since, $Y_{n+\frac{1}{2}}(kr)$ has infinite value at $r=0$, any linear combination of $J_{n+\frac{1}{2}}(kr)$ and $Y_{n+\frac{1}{2}}(kr)$ also has finite value at $r=0$. But at $r=0$ the field vectors have finite values. Therefore, the acceptable solution of Eq. (D.32) is of the form,

$$X(r) \sim J_{n+\frac{1}{2}}(kr) \quad (D.33)$$

Thus, the form of $R(r)$ is given by, $R(r) \sim J_{n+\frac{1}{2}}(kr)/\sqrt{r}$ and therefore, one can write the expression for ψ as,

$$\psi(r, \theta, \phi) \sim \frac{1}{\sqrt{kr}} J_{n+\frac{1}{2}}(kr) P_n^m(\cos \theta) \cos m\phi \quad (D.34)$$

In the expression (D.34) A is a constant which can be determined from the boundary conditions. Here we have dropped the $\sin m\phi$ term without any loss of generality. Since ψ is a single valued function, it must take the same value for ϕ and $\phi + 2\pi$. So $\cos m\phi = \cos(m\phi + 2\pi) = \cos(m\phi + 2m\pi) = \cos m\phi$ only when $m = 0, \pm 1, \pm 2, \pm 3, \dots$ i.e., m takes integral values only. This same requirement limits n also to integral values only. Negative values of m give the same field distributions as positive and hence, do not provide separate solutions. Similarly, negative values of n also do not produce extra solutions. The constant m must be less than or equal to n . The possibilities that the constant n can or cannot take value as 0. However, m can always take 0 value and it gives rotational symmetry about the diameter of a sphere joining the points $\theta = 0^\circ$ and $\theta = 180^\circ$.

Using the expression for (r, θ, ϕ) from Eq. (D.34), one can find out the expression for the field components for the $TE_{nm\ell}$ and the $TM_{nm\ell}$ modes.

D.D.(1) Field expressions for the $TM_{nm\ell}$ modes

Using expression for ψ from Eq. (D.34) the electric field components for the $TE_{nm\ell}$ modes can be determined using Eq. (D.22) and the expression of $\nabla \psi$ which is given as,

$$\nabla \psi = \hat{r} \frac{\partial \psi}{\partial r} + \hat{\theta} \frac{1}{r} \frac{\partial \psi}{\partial \theta} + \hat{\phi} \frac{1}{r \sin \theta} \frac{\partial \psi}{\partial \phi} \quad (D.35)$$

Using Eq. (D.35), the electric field \vec{E} is determined as follows,

$$\begin{aligned} \vec{E} &= \vec{r} \times \nabla \psi \\ \nabla \psi &= \begin{vmatrix} \hat{r} & \hat{\theta} & \hat{\phi} \\ r & 0 & 0 \\ \frac{\partial \psi}{\partial r} & \frac{1}{r} \frac{\partial \psi}{\partial \theta} & \frac{1}{r \sin \theta} \frac{\partial \psi}{\partial \phi} \end{vmatrix} \\ &= -\frac{1}{\sin \theta} \frac{\partial \psi}{\partial \phi} \hat{\theta} + \frac{\partial \psi}{\partial \theta} \hat{\phi} \end{aligned} \quad (D.36)$$

Now expressing \vec{E} by,

$$\vec{E} = \hat{r} E_r + \hat{\theta} E_\theta + \hat{\phi} E_\phi \quad (D.37)$$

and comparing the components from Eqs. (D.36) and (D.37) we get,

$$E_r = 0 \quad (D.38)$$

$$E_\theta = -\frac{1}{\sin \theta} \frac{\partial \psi}{\partial \phi} \quad (D.39)$$

$$E_\phi = \frac{\partial \psi}{\partial \theta} \quad (D.40)$$

Substituting the value of ψ from Eq. (D.34) in Eqs. (D.38)-(D.40) we get,

$$E_r = 0 \quad (D.41)$$

$$E_\theta = \frac{mA}{\sqrt{kr} \sin \theta} J_{n+\frac{1}{2}}(kr) P_n^m(\cos \theta) \sin m\phi \quad (D.42)$$

$$E_\phi = \frac{A}{\sqrt{kr}} J_{n+\frac{1}{2}}(kr) \frac{d}{d\theta} \{P_n^m(\cos \theta)\} \cos m\phi \quad (D.43)$$

Alternatively, introducing the angular momentum operator \vec{L} defined by $\vec{L} = \frac{1}{j} (\vec{r} \times \nabla)$, where $j = \sqrt{-1}$ and constructing L^2 and using its relationship with the Laplacian operator (∇^2), the solution for the TE mode can be constructed following [39-40]. The above method and the method used earlier to find solution (Eqs. (D.41)-(D.43)) yield equivalent results as can be verified from the field expressions (Eqs. (D.41)-(D.43)) and the ones given [39-40].

Now substituting the value of E_r, E_θ and E_ϕ from Eqs. (D.41)-(D.43) into Eqs. (D.12)-(D.14), one obtains expressions for H_r, H_θ and H_ϕ . The RHS of Eq. (D.12) involves E_θ and E_ϕ and substituting the values of E_θ and E_ϕ from Eqs. (D.41) and (D.43) it yields,

$$\begin{aligned} H_r &= -\frac{A J_{n+\frac{1}{2}}(kr) \cos m\phi}{j\omega \mu_0 r \sqrt{kr}} \times \left[\sin^2 \theta \frac{d^2}{d\theta^2} \{P_n^m(\cos \theta)\} \right. \\ &\quad \left. - 2 \cos \theta \frac{d}{d\theta} \{P_n^m(\cos \theta)\} - \frac{m^2}{\sin^2 \theta} \{P_n^m(\cos \theta)\} \right] \end{aligned} \quad (D.44)$$

Using recurrence relation for $P_n^m(\cos \theta)$ [Appendix-B, Eqs. (B10) and (B11)] the term within the square bracket of Eq. (D.44) is simplified to give $-n(n+1) P_n^m(\cos \theta)$.

Therefore, the expression for H_r becomes

$$H_r = \frac{n(n+1)A}{j\omega \mu_0 r \sqrt{kr}} J_{n+\frac{1}{2}}(kr) P_n^m(\cos \theta) \cos m\phi \quad (D.45)$$

To get the expression for E_θ and E_ϕ is straightforward, as RHSs of Eqs. (D.13) and (D.14) involve E_r which vanishes for the $TE_{nm\ell}$ mode leaving single term for these equations. The expression for H_θ and H_ϕ are determined as

$$H_\theta = \frac{A}{j\omega \mu_0 r \sqrt{k}} \frac{d}{dr} \{ \sqrt{r} J_{n+\frac{1}{2}}(kr) \} \frac{d}{d\theta} \{ P_n^m(\cos \theta) \} \cos m\phi \quad (D.46)$$

$$H_\phi = -\frac{mA}{j\omega \mu_0 r \sin \theta \sqrt{k}} \frac{d}{dr} \{ \sqrt{r} J_{n+\frac{1}{2}}(kr) \} \frac{d}{d\theta} \{ P_n^m(\cos \theta) \} \sin m\phi \quad (D.47)$$

Supplementary materials

Supplementary material associated with this article can be found, in the online version, at doi:10.1016/j.jqsrt.2018.12.001.

References

- [1] Debye P. Der lichtdruck auf kugeln von beliebigem material. Ann Phys 1909;30:57.
- [2] Lorenz L. Sur. La. Lumiere reflexie et refractee purune sphere transparente.. In: Oeuvres scientifiques de L. Lorenz, revues et annotees par H. Valentiner Lehmann et stage; 1898. p. 405.
- [3] Lorenz L. Lysbevaegelsemioguden for en haf plane lysbolger belystkulge. Vidensk Selk Skr 1890;6:1.
- [4] Mie G. Beitrage zur optik truber medien, speziell kolloidaler metallosungen. Ann Phys 1908;25:377.
- [5] Affolter P, Eliasson B. Electromagnetic resonance and Q factor of lossy dielectric sphere. IEEE Trans Microwave Theory Tech 1973;21:573-8 and references cited therein.
- [6] Ashkin A, Dziedzic JM. Observation of resonances in the radiation pressure on dielectric spheres. Phys Rev Lett 1977;38:1351-4.
- [7] Bennet HS, Rosasco GJ. Appl Opt 1978;17:491.

- [8] Chylek P, Kiehl JT, Ko MKW. Narrow resonance structure in the my scattering characteristic. *Appl Opt* 1978;17:3019–21.
- [9] Chylek P, Kiehl JT, Ko MKW. Optical levitation and partial wave resonance. *Phys Rev A* 1978;18:2229–33.
- [10] Stein SR, Turneare JP. In: Proc. 27th Annu. Symp. Frequency Control (Washington, DC: Electrical Industries Association; 1973. p. 414–20.
- [11] Strayer DM, Dick GJ, Tward E. *IEEE Trans Magn* 1983;512.
- [12] Mann AG, Blair DG. *J Phys D* 1983;16:105.
- [13] Jimenez JJ, Septier A. In: Proc. 27th annu. symp. frequency control. Washington, DC: Electrical Industries Association; 1973. p. 406–13.
- [14] Braginsky VB, Panov VI, Vasiliiev SI. *IEEE Trans Magn* 1981;955–62.
- [15] Braginsky VB, Panov VI, Timashov AV. *Sov Phys-Dokl* 1982;267.
- [16] Tomassetti G, Weinreb S, Wellington K. *Electron Lett* 1981;17:949–1000.
- [17] Thakoor S, Strayer DM, Dick GJ, Mercereau JE. *J Appl Phys* 1986;59:854–62.
- [18] Cohn SB. Microwave band pass filters containing high-Q dielectric resonator. *IEEE Trans Microwave Theory Tech* 1969 (April(4)):218–27.
- [19] Kobayashi Y, Tanaka S. Resonant mode of a dielectric rod resonator short-circuited at both ends by parallel conducting plates. *IEEE Trans Microwave Theory Tech* 1980 (October(10)):1077–85.
- [20] Zaki KA, Atia AE. Modes in dielectric-loaded waveguides and resonators. *IEEE Trans Microwave Theory Tech* 1986 (July(7)):815–24.
- [21] Glisson AW, Kajfez D, James J. Evaluation of modes in dielectric resonators using a surface integral equation formulation. *IEEE Trans Antennas Propagat* 1983 (December(12)):1023–9.
- [22] De Smedt R. Correction due to a finite permittivity for a ring resonator in free space. *IEEE Trans Microwave Theory Tech*. 1984;32 (October(10)):1288–93.
- [23] Hernandez-Gil F, Martinez JP. Analysis of dielectric resonators with tuning screw and supporting structure. *IEEE Trans Microwave Theory Tech* 1985 (December(12)):1453–7.
- [24] Lee JF, Wilkins GM, Mittra R. Finite-element analysis of axisymmetric cavity resonator using a hybrid edge element technique. *IEEE Trans Microwave Theory Tech* 1993 (November(11)):1981–6.
- [25] Wong MF, Prak M, Hanna VF. Axisymmetric edge-based finite element formulation for bodies of revolution: Application to dielectric resonators. In: *IEEE MTT-S Int. Microwave Symp. Dig. orlando*; May 1995. p. 285–8.
- [26] Greenwood AD, Jin JM. A novel efficient algorithm for scattering from a complex BOR using mixed finite elements and cylindrical PML. *IEEE Trans Antennas Propagat* 1999;47 (April(4)):620–9.
- [27] Kobayashi Y, Senju T. Resonant modes in shielded uniaxial - anisotropic dielectric rod resonators. *IEEE Trans Microwave Theory Tech* 1993;41 (December(12)):2198–205.
- [28] Guan JM, Su CC. Resonant frequencies and field distributions for the shielded uniaxially anisotropic dielectric resonator by th FD-SIC method. *IEEE Trans Microwave Theory Tech* 1997;45 (October(10)):1767–77.
- [29] Krupa J, Cross D, Aubourg M, Guillon P. Study of Whispering gallery modes in anisotropic single-crystal dielectric resonators. *IEEE Trans Microwave Theory Tech* 1994;42 (January(1)):55–61.
- [30] Krupa J, Derzakowski K, Abramowicz A, Tobar ME, Geyer RG. Use of whispering-gallery modes for complex permittivity determinations of ultra-low-loss dielectric materials. *IEEE Trans Microwave Theory Tech*. 1999;47 (June(6)):752–9.
- [31] Wang C, Zaki KA. Generalized multilayer anisotropic dielectric resonators. *IEEE Trans Microwave Theory Tech* 2000;48 (January(1)):60–6.
- [32] Mongia RK, Bhartia P. Accurate conductor Q-factor of dielectric resonator placed in an MIC environment. *IEEE Trans Microwave Theory Tech* 1993;41 (March(3)):445–9.
- [33] Guan JM, Su CC. Precise computations of resonant frequencies and quality factors for dielectric resonators in MIC's with tuning elements. *IEEE Trans Microwave Theory Tech* 1997;45 (March(3)):439–42.
- [34] Shen T, Zaki KA, Wang C. Tunable dielectric resonators with dielectric tuning disks. *IEEE Trans Microwave Theory Tech* 2000;48 (December(12)):2439–45.
- [35] Hui WK, Wolff I. A multicomposite, multilayered cylindrical dielectric resonator for application in MMIC's. *IEEE Trans Microwave Theory Tech* 1994;42 (March(3)):415–23.
- [36] Kharkovsky S, Filipov Y, Eremenko Z. Whispering gallery modes of an open hemispherical image dielectric resonator. *Microwave Opt Technol Lett* 1999;21 (May):252–7.
- [37] Baumann D, Fumeaux C, Leuchtmann P, Vahldieck R. Finite- volume time-domain (FVTD) method and its application to the analysis of hemispherical dielectric-resonator antennas. In: *IEEE MTT-S int. microwave symp. dig.*; Jun. 2003. p. 985–8.
- [38] Gil JM. CAD-oriented Analysis of Cylindrical and Spherical dielectric resonators in cavities and MIC Environments by means of finite Elements. *IEEE Trans Microwave Theory Tech* 2005;53:1–9.
- [39] Yadav RA, Singh ID. Normal modes and quality factors of dielectric spherical resonators: I shielded dielectric spherical resonators. *Pramana* 2004;62:1255.
- [40] Yadav RA, Yadav TK, Maurya MK, Yadav DP, Singh NP. Normal modes and quality factors of shielded composite dielectric spherical resonators. *Indian J Phys* 2009;83:1421–38.
- [41] Yadav DP, Maurya MK, Yadav RA, Singh NP. Resonant and normal modes behavioral studies of shielded dielectric spherical shell resonator. *Optik* 2016;127:5520–33.